

Lectures on Diffraction and Saturation of Nuclear Partons in DIS off Heavy Nuclei ¹

I.P. Ivanov^a, N.N. Nikolaev^{b,c)}, W. Schäfer^{b)}, B.G. Zakharov^{c)}
 & V.R. Zoller^{d)}

^{a)} *Institute of Mathematics, Novosibirsk, Russia*

^{b)} *Institut f. Kernphysik, Forschungszentrum Jülich, D-52425 Jülich, Germany*

^{c)} *L.D.Landau Institute for Theoretical Physics, Chernogolovka, Russia*

^{d)} *Institute for Theoretical and Experimental Physics, Moscow, Russia*

E-mail: N.Nikolaev@fz-juelich.de

Abstract

The Lorentz contraction of ultrarelativistic nuclei entails a spatial overlap and fusion (recombination, saturation) of partons belonging to different nucleons at the same impact parameter. In these lectures we present a consistent description of the fusion of partons in terms of nuclear attenuation of color dipole states of the photon and collective Weizsäcker-Williams (WW) gluon structure function of a nucleus. The point that all observables for DIS off nuclei are uniquely calculable in terms of the nuclear WW glue amounts to a new form of factorization in the saturation regime.

We start with the theory of multichannel propagation of color dipoles in a nuclear medium including the color-singlet to color-octet to color-octet transitions. We show how the Glauber-Gribov formulas are recovered from the multichannel formalism. Then we derive the two-plateau momentum distribution of final state (FS) quarks produced in deep inelastic scattering (DIS) off nuclei in the saturation regime. The diffractive plateau which dominates for small \mathbf{p} measures precisely the momentum distribution of quarks in the beam photon, the rôle of the nucleus is simply to provide an opacity. The plateau for truly inelastic DIS exhibits a substantial nuclear broadening of the FS momentum distribution. The Weizsäcker-Williams glue of a nucleus exhibits a substantial nuclear dilution, still soft initial state (IS) nuclear sea saturates because of the anti-collinear splitting of gluons into sea quarks. Then we comment on the signatures of saturation in exclusive diffractive DIS.

A large body of these lectures is on the recent theory of jet-jet inclusive cross sections. We show that for hard dijets the decorrelation momentum is of the order of the nuclear saturation momentum Q_A . For minijets with the transverse momentum below the saturation scale we predict a complete disappearance of the azimuthal jet-jet correlation. We conclude with comment on a possible relevance of the decorrelation of jets to the experimental data from the STAR-RHIC Collaboration.

¹The notes of lectures presented by N.N.N. at the XXXVI St.Petersburg Nuclear Physics Institute Winter School on Nuclear and Particle Physics & VIII St.Petersburg School on Theoretical Physics, St.Petersburg, Repino, February 25 - March 3, 2002

1 Introduction

Within the standard QCD parton model the virtual photoabsorption cross section is proportional to the density of partons in the target. Inverting the argument, one would define the density of partons in a target A as

$$F_2(x, Q^2) = \sum_f e_f^2 [q_f(x, Q^2) + \bar{q}_f(x, Q^2)] = \frac{Q^2}{4\pi^2 \alpha_{em}} \sigma_{\gamma^* A} \quad (1)$$

In the so-called brick-wall or Breit frame, in which the photon has a zero energy and the (target) hadron or nucleus is ultrarelativistic, DIS amounts to backward reflection of the parton with the longitudinal momentum $k_z = xP_z = \frac{1}{2}q_z = \frac{1}{2}\sqrt{Q^2}$, see fig.1.

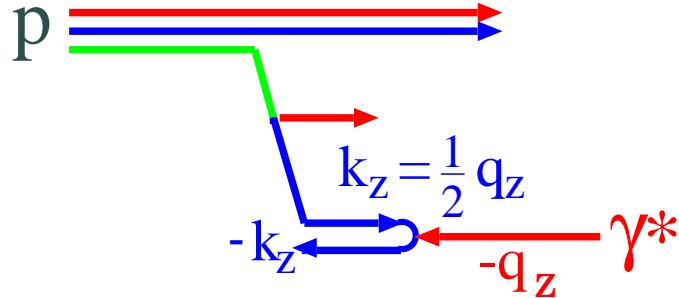


Figure 1: *DIS in the Breit frame*

When DIS is viewed in the laboratory frame, the hadronic properties of photons suggest [1] a nuclear shadowing by which the density of partons in a nucleus rises slower than $\propto A$. Very heavy nuclei will be opaque to a part of the Fock states of the photon [2]. When viewed in the Breit frame, the Lorentz contraction of an ultrarelativistic nucleus entails a spatial overlap and fusion of partons at

$$x \lesssim x_A = \frac{1}{R_A m_N} \quad (2)$$

as indicated in fig. 2.

This interpretation of nuclear opacity in terms of a fusion and saturation of nuclear partons has been introduced in 1975 [1] way before the QCD parton model. The review of early works on nuclear shadowing can be found in lectures by one of the authors at the 1976 Winter School of PNPI [3], see also [4]. The pQCD link between nuclear opacity and saturation has been considered in ref. [5] and by Mueller [6], the pQCD discussion of fusion of nuclear gluons has been revived by McLerran et al. [7].

The common wisdom is that in DIS the final state (FS) interaction of the struck parton, which in the Breit frame moves in the direction opposite to the debris of the nucleon/nucleus, see fig. 2, can be neglected and the observed transverse and longitudinal momentum distribution of struck partons in the FS coincides with the initial state (IS) density of partons in the probed hadron. Based on the consistent treatment of intranuclear

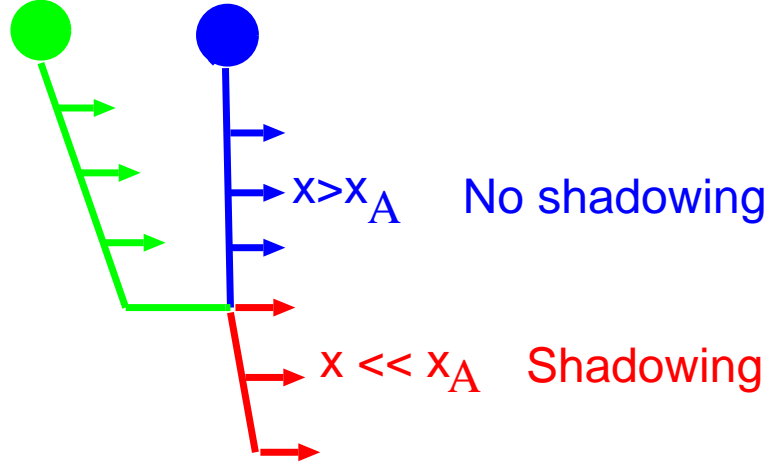


Figure 2: *The fusion of partons from overlapping parton clouds of two nucleons in a Lorentz-contracted nucleus*

distortions, we derive the two-plateau spectrum of FS quarks found in [8]. Following our early analysis of diffractive DIS off nucleons [9, 10] and nuclei [11], we introduce the collective Weizsäcker-Williams gluon structure function of the nucleus, which uniquely defines all nuclear DIS observables. We find a substantial nuclear broadening of inclusive FS spectra and demonstrate that despite this broadening the FS sea parton density exactly equals the IS sea parton density calculated in terms of the WW glue of the nucleus as defined according to [11]. We pay special attention to an important point that diffractive DIS in which the target nucleus does not break and is retained in the ground state, makes precisely 50 per cent of the total DIS events for heavy nuclei at small x [2]. We point out that the saturated diffractive plateau measures precisely the momentum distribution of (anti-)quarks in the $q\bar{q}$ Fock state of the photon. In contrast to DIS off nuclei, the fraction of DIS off free nucleons which is diffractive, and which also measures unitarity corrections to the two-gluon exchange approximation [12, 13], is negligibly small [14], $\eta_D \lesssim 6\text{-}10\%$, and there is little room for genuine saturation effects even at HERA. We show how the anti-collinear splitting of WW gluons into sea quarks gives rise to nuclear saturation of the sea despite a substantial nuclear dilution of the WW glue.

After establishing the properties of the single-jet inclusive cross section, we turn our attention to the recent theory of jet-jet (de)correlations [15]. After a hard scattering partons with large transverse momentum fragment into a high-energy jet of particles. In deep inelastic scattering at small x , to the collinear approximation, the photon-gluon fusion $\gamma^*g \rightarrow q\bar{q}$, often referred to as an interaction of the unresolved photon, gives rise to the back-to-back jets in the current or photon fragmentation region. The experimental signature of the unresolved photon interaction is that the so-called lightcone plus-components of the jet momenta sum up to the lightcone plus-component of the photon's momentum. The allowance for the transverse momentum of gluons leads to the disparity of the momenta and azimuthal decorrelation of the quark and antiquark jets, which within the k_\perp -factorization can be quantified in terms of the so-called unintegrated gluon structure function of the target (see [16] and references therein).

In view of the substantial nuclear broadening of the unintegrated gluon SF of nuclei it is natural to expect stronger azimuthal decorrelation of jets produced in DIS off nuclei. In these lectures we report a consistent multiple-scattering theory of jet-jet decorrelation in the genuinely inelastic DIS followed by color excitation of the target nucleus. For heavy nuclei of equal importance is coherent diffractive DIS in which the target nucleus does not break and is retained in the ground state. In these coherent diffractive events quark and antiquark jets are produced exactly back-to-back with negligibly small transverse decorrelation momentum

$$|\Delta| = |\mathbf{p}_+ + \mathbf{p}_-| \lesssim 1/R_A \sim m_\pi/A^{1/3}, \quad (3)$$

where R_A is the radius of the target nucleus. For hard jets diffractive attenuation effects are weak and we report a compact formula for the broadening of azimuthal correlations between the quark and antiquark jets. In this case the decorrelation (acoplanarity, out-of-plane) momentum is given by the nuclear saturation momentum Q_A . Then we prove a disappearance of the jet-jet correlation for minijets with the transverse momentum below the saturation scale Q_A . In the Conclusions we summarize our principal findings and speculate on their relevance to the recent observation of the dissolution of the away jets in central nuclear collisions at RHIC [17].

2 Quark and antiquark jets in DIS off free nucleons: single particle spectrum and jet-jet decorrelation

We recall briefly the color dipole formulation of DIS [2, 5, 9, 19, 12, 18] and illustrate our ideas on an example of jet-jet decorrelation in DIS off free nucleons which at moderately small x is dominated by interactions of $q\bar{q}$ states of the photon. We evaluate the jet production cross section at the parton level. The total cross section for interaction of the color dipole \mathbf{r} with the target nucleon equals

$$\begin{aligned} \sigma(r) &= \alpha_S(r)\sigma_0 \int d^2\kappa f(\kappa) [1 - \exp(i\kappa\mathbf{r})] \\ &= \frac{1}{2}\alpha_S(r)\sigma_0 \int d^2\kappa f(\kappa) [1 - \exp(i\kappa\mathbf{r})] \cdot [1 - \exp(-i\kappa\mathbf{r})], \end{aligned} \quad (4)$$

where $f(\kappa)$ is related to the unintegrated glue of the target nucleon by

$$f(\kappa) = \frac{4\pi}{N_c\sigma_0} \cdot \frac{1}{\kappa^4} \cdot \frac{\partial G}{\partial \log \kappa^2} \quad (5)$$

and is normalized as

$$\int d^2\kappa f(\kappa) = 1. \quad (6)$$

For DIS off a free nucleon target, see figs. 3a-3d, the total photoabsorption cross section equals

$$\sigma_N = \int d^2\mathbf{r} dz |\Psi(z, \mathbf{r})|^2 \sigma(\mathbf{r}). \quad (7)$$

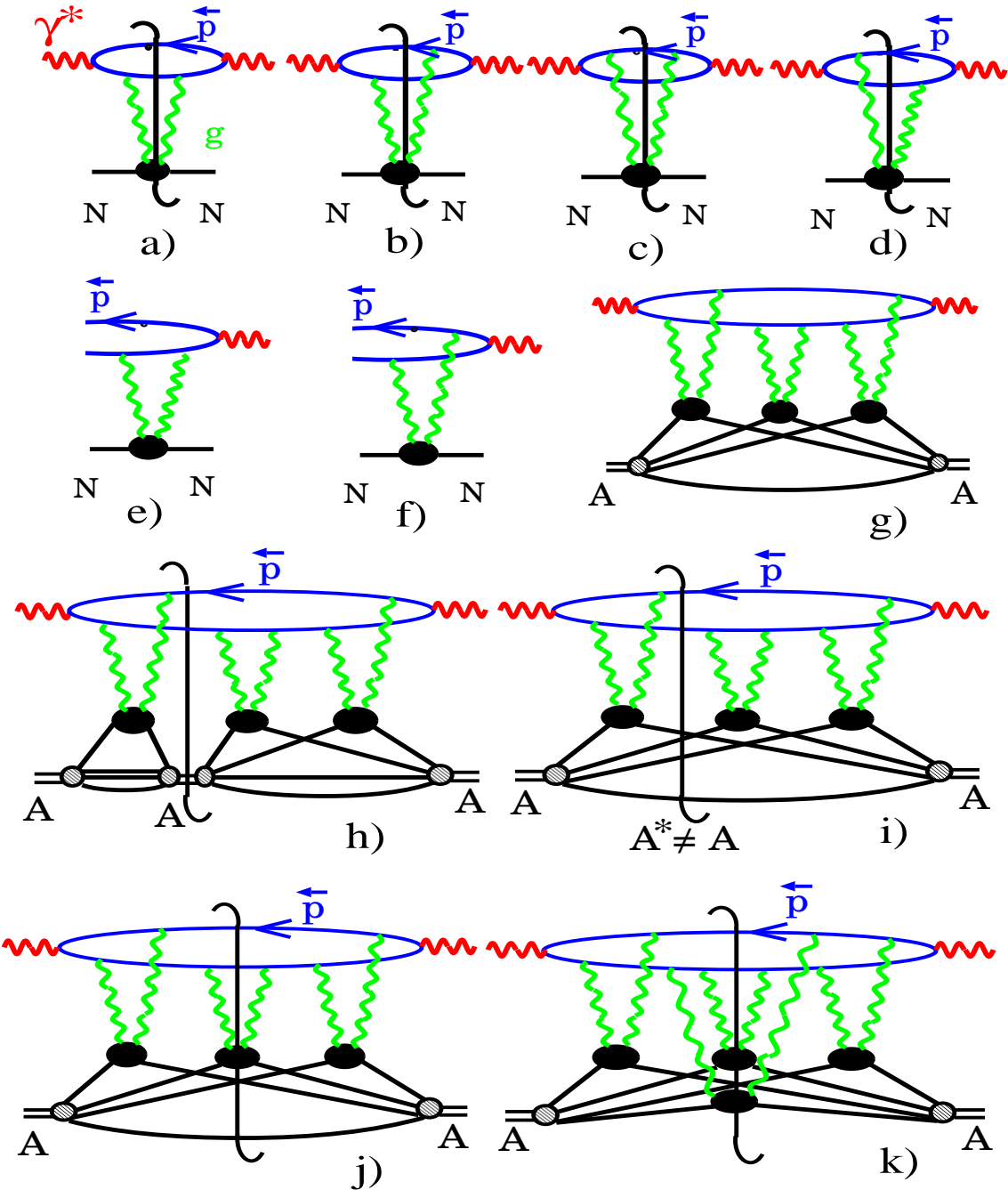


Figure 3: The p QCD diagrams for inclusive (a-d) and diffractive (e,f) DIS off protons and nuclei (g-k). Diagrams (a-d) show the unitarity cuts with color excitation of the target nucleon, (g) - a generic multiple scattering diagram for Compton scattering off nucleus, (h) - the unitarity cut for a coherent diffractive DIS, (i) - the unitarity cut for quasielastic diffractive DIS with excitation of the nucleus A^* , (j,k) - the unitarity cuts for truly inelastic DIS with single and multiple color excitation of nucleons of the nucleus.

Upon the relevant Fourier transformations one finds the momentum spectrum of the final state (FS) quark prior the hadronization,

$$\frac{d\sigma_N}{d^2\mathbf{p} dz} = \frac{\sigma_0}{2} \cdot \frac{\alpha_S(\mathbf{p}^2)}{(2\pi)^2} \int d^2\boldsymbol{\kappa} f(\boldsymbol{\kappa}) |\langle \gamma^* | \mathbf{p} \rangle - \langle \gamma^* | \mathbf{p} - \boldsymbol{\kappa} \rangle|^2 \quad (8)$$

where \mathbf{p} is the transverse momentum of the quark and $z_+ = z$ and $z_- = 1 - z$ are the fractions of photon's lightcone momentum carried by the quark and antiquark, respectively. The variables z_\pm for the observed jets add up to unity which is the signature of the unresolved photon interaction.

For the reference, we cite here the relevant overlap of the momentum space wave functions of the photon, summed over the helicities of the FS quark and antiquark [5]. For transverse photons

$$\begin{aligned} & (\langle \gamma^* | \mathbf{p} \rangle - \langle \gamma^* | \mathbf{p} - \boldsymbol{\kappa} \rangle) \cdot (\langle \mathbf{p} | \gamma^* \rangle - \langle \mathbf{p} - \boldsymbol{\kappa} | \gamma^* \rangle) \Big|_{\lambda_\gamma=\pm 1} = \\ & 2N_c e_f^2 \alpha_{em} \times \left\{ [z^2 + (1-z)^2] \left(\frac{\mathbf{p}}{\mathbf{p}^2 + \varepsilon^2} - \frac{\mathbf{p} - \boldsymbol{\kappa}}{(\mathbf{p} - \boldsymbol{\kappa})^2 + \varepsilon^2} \right) \right. \\ & \quad \cdot \left. \left(\frac{\mathbf{p}}{\mathbf{p}^2 + \varepsilon^2} - \frac{\mathbf{p} - \boldsymbol{\kappa}}{(\mathbf{p} - \boldsymbol{\kappa})^2 + \varepsilon^2} \right) \Big|_{\lambda+\bar{\lambda}=0} \right. \\ & \quad + m_f^2 \left(\frac{1}{\mathbf{p}^2 + \varepsilon^2} - \frac{1}{(\mathbf{p} - \boldsymbol{\kappa})^2 + \varepsilon^2} \right) \\ & \quad \cdot \left. \left(\frac{1}{\mathbf{p}^2 + \varepsilon^2} - \frac{1}{(\mathbf{p} - \boldsymbol{\kappa})^2 + \varepsilon^2} \right) \Big|_{\lambda+\bar{\lambda}=\lambda_\gamma} \right\} \end{aligned} \quad (9)$$

and for the longitudinal photons

$$\begin{aligned} & (\langle \gamma^* | \mathbf{p} \rangle - \langle \gamma^* | \mathbf{p} - \boldsymbol{\kappa} \rangle) \cdot (\langle \mathbf{p} | \gamma^* \rangle - \langle \mathbf{p} - \boldsymbol{\kappa} | \gamma^* \rangle) \Big|_{\lambda_\gamma=0} \\ & = 8N_c e_f^2 \alpha_{em} Q^2 z^2 (1-z)^2 \\ & \times \left(\frac{1}{\mathbf{p}^2 + \varepsilon^2} - \frac{1}{(\mathbf{p} - \boldsymbol{\kappa})^2 + \varepsilon^2} \right) \cdot \left(\frac{1}{\mathbf{p}^2 + \varepsilon^2} - \frac{1}{(\mathbf{p} - \boldsymbol{\kappa})^2 + \varepsilon^2} \right) \Big|_{\lambda+\bar{\lambda}=\lambda_\gamma} \end{aligned} \quad (10)$$

where

$$\varepsilon^2 = z(1-z)Q^2 + m_f^2 \quad (11)$$

and m_f is the mass of the quark q_f with the charge e_f . Now, notice that the transverse momentum of the gluon is precisely the decorrelation momentum Δ , so that in the still further differential from

$$\frac{d\sigma_N}{dz d^2\mathbf{p}_+ d^2\Delta} = \frac{\sigma_0}{2} \cdot \frac{\alpha_S(\mathbf{p}^2)}{(2\pi)^2} f(\Delta) |\langle \gamma^* | \mathbf{p}_+ \rangle - \langle \gamma^* | \mathbf{p}_+ - \Delta \rangle|^2 \quad (12)$$

A useful small- Δ expansion for light flavors is

$$\begin{aligned} \frac{d\sigma_N}{dz d^2\mathbf{p}_+ d^2\Delta} &= \frac{N_c e_f^2 \alpha_{em} \sigma_0 \alpha_S(\mathbf{p}^2)}{(2\pi)^2} [z^2 + (1-z)^2] \\ &\times f(\Delta) \left\{ \left[\frac{\varepsilon^2 - \mathbf{p}_+^2}{(\varepsilon^2 + \mathbf{p}_+^2)^2} \right]^2 \Delta_L^2 + \left[\frac{1}{\varepsilon^2 + \mathbf{p}_+^2} \right]^2 \Delta_\perp^2 \right\} \end{aligned} \quad (13)$$

where Δ_L and Δ_\perp are the components of the decorrelation parallel, and transverse, to \mathbf{p}_+ . Only the latter, acoplanarity component, contributes to the azimuthal jet-jet decorrelation, the former is only measurable if full experimental reconstruction of jets is possible. This is the leading order result from the k_\perp factorization, for the applications to DIS off free nucleons see [16] and references therein. Below we shall extend (12) to jet-jet inclusive cross section for interactions of unresolved photons with nuclear targets.

3 Propagation of color dipoles in nuclear medium

We focus on DIS at $x \lesssim x_A = 1/R_A m_N \ll 1$ which is dominated by interactions of $q\bar{q}$ states of the photon. Extension to interactions of higher Fock states of the photon is straightforward and will give rise to the evolution effects, which we do not consider here. For $x \lesssim x_A$ the propagation of the $q\bar{q}$ pair inside nucleus can be treated in the straight-path approximation.

We work in the conventional approximation of two t-channel gluons in DIS off free nucleons. The relevant unitarity cuts of the forward Compton scattering amplitude are shown in fig. 3a-3d and describe the transition from the color-neutral $q\bar{q}$ dipole to the color-octet $q\bar{q}$ pair. (Really, for $SU(N_c)$ we have fundamental & adjoint multiplets instead of the triplet & octet familiar for $N_c = 3$, our continuous reference to the latter should not cause any confusion.) The two-gluon exchange approximation amounts to neglecting small unitarity corrections to DIS off free nucleons [12, 13], which are quantified by diffractive DIS described by higher order diagrams of fig. 3e,3f. This approximation is justified by a small fraction of diffractive DIS, $\eta_D \ll 1$ [14]. The unitarity cuts of the nuclear Compton scattering amplitude which correspond to the genuine inelastic DIS with color excitation of the nucleus are shown in figs. 3j,3k. Here we notice that in the diagram 3k the $q\bar{q}$ pair propagates in the both color-octet and color-singlet states.

Let \mathbf{b}_+ and \mathbf{b}_- be the impact parameters of the quark and antiquark, respectively, and $S_A(\mathbf{b}_+, \mathbf{b}_-)$ be the S-matrix for interaction of the $q\bar{q}$ pair with the nucleus. We are interested in the inclusive cross section when we sum over all excitations of the target nucleus when one or several nucleons have been color excited. A convenient way to sum such cross sections is offered by the closure relation. Regarding the color states c_{km} of the $q_k \bar{q}_m$ pair, we sum over all octet and singlet states. Then, the the 2-body inclusive spectrum is calculated in terms of the 2-body density matrix as

$$\begin{aligned} \frac{d\sigma_{in}}{dz d^2\mathbf{p}_+ d^2\mathbf{p}_-} &= \frac{1}{(2\pi)^4} \int d^2\mathbf{b}'_+ d^2\mathbf{b}'_- d^2\mathbf{b}_+ d^2\mathbf{b}_- \\ &\times \exp[-i\mathbf{p}_+(\mathbf{b}_+ - \mathbf{b}'_+) - i\mathbf{p}_-(\mathbf{b}_- - \mathbf{b}'_-)] \\ &\times \Psi^*(\mathbf{b}'_+ - \mathbf{b}'_-) \Psi(\mathbf{b}_+ - \mathbf{b}_-) \\ &\times \left\{ \sum_{A^*} \sum_{km} \langle 1; A | S_A^*(\mathbf{b}'_+, \mathbf{b}'_-) | A^*; c_{km} \rangle \langle c_{km}; A^* | S_A(\mathbf{b}_+, \mathbf{b}_-) | A; 1 \rangle \right. \\ &\quad \left. - \langle 1; A | S_A^*(\mathbf{b}'_+, \mathbf{b}'_-) | A; 1 \rangle \langle 1; A | S_A(\mathbf{b}_+, \mathbf{b}_-) | A; 1 \rangle \right\} \end{aligned} \quad (14)$$

Here Ψ is the $q\bar{q}$ -Fock state wave function of the virtual photon, and we suppressed its dependence on z_\pm . In the integrand of (14) we subtracted the diffractive component of the

final state. Notice, that the four straight-path trajectories $\mathbf{b}_\pm, \mathbf{b}'_\pm$ enter the calculation of the full fledged 2-body density matrix and S_A and S_A^* describe the propagation of two $q\bar{q}$ pairs inside a nucleus.

Upon the application of closure to sum over nuclear final states A^* the integrand of (14) can be considered as an intranuclear evolution operator for the 2-body density matrix (for the related discussion see ref. [20])

$$\begin{aligned} \sum_{A^*} \sum_{km} \langle A | \left\{ \langle 1 | S_A^*(\mathbf{b}'_+, \mathbf{b}'_-) | c_{km} \rangle \right\} | A^* \rangle \langle A^* | \left\{ \langle c_{km} | S_A(\mathbf{b}_+, \mathbf{b}_-) | 1 \rangle \right\} | A \rangle = \\ = \langle A | \left\{ \sum_{km} \langle 1 | S_A^*(\mathbf{b}'_+, \mathbf{b}'_-) | c_{km} \rangle \langle c_{km} | S_A(\mathbf{b}_+, \mathbf{b}_-) | 1 \rangle \right\} | A \rangle \end{aligned} \quad (15)$$

Let the QCD eikonal for the quark-nucleon and antiquark-nucleon one-gluon exchange interaction be $T_+^a \Delta(\mathbf{b})$ and $T_-^a \Delta(\mathbf{b})$, where T_+^a and T_-^a are the $SU(N_c)$ generators for the quark and antiquark states, respectively. The vertex V_a for excitation of the nucleon $g^a N \rightarrow N_a^*$ into color octet state is so normalized that after application of closure the vertex $g^a g^b NN$ in the diagrams of fig. 3a-3d is δ_{ab} . Then, to the two-gluon exchange approximation, the S -matrix of the $(q\bar{q})$ -nucleon interaction equals

$$S_N(\mathbf{b}_+, \mathbf{b}_-) = 1 + i[T_+^a \Delta(\mathbf{b}_+) + T_-^a \Delta(\mathbf{b}_-)]V_a - \frac{1}{2}[T_+^a \Delta(\mathbf{b}_+) + T_-^a \Delta(\mathbf{b}_-)]^2 \quad (16)$$

and the color-dipole cross section for the $q\bar{q}$ dipole is

$$\sigma(\mathbf{b}_+ - \mathbf{b}_-) = \frac{N_c^2 - 1}{2N_c} \int d^2 \mathbf{b}_+ [\Delta(\mathbf{b}_+) - \Delta(\mathbf{b}_-)]^2. \quad (17)$$

The nuclear S -matrix of the straight-path approximation is given by

$$S_A(\mathbf{b}_+, \mathbf{b}_-) = \prod_{j=1}^A S_N(\mathbf{b}_+ - \mathbf{b}_j, \mathbf{b}_- - \mathbf{b}_j) \quad (18)$$

where \mathbf{b}_j are the transverse coordinates of nucleons in a nucleus and the ordering along the longitudinal path is understood. We evaluate the nuclear expectation value in (15) in the standard dilute gas approximation. To the two-gluon exchange approximation, only the terms quadratic in $\Delta(\mathbf{b}_j)$ must be kept in the evaluation of the single-nucleon matrix element

$$\langle N_j | S_N^*(\mathbf{b}'_+ - \mathbf{b}_j, \mathbf{b}'_- - \mathbf{b}_j) S_N(\mathbf{b}_+ - \mathbf{b}_j, \mathbf{b}_- - \mathbf{b}_j) | N_j \rangle$$

per each and every nucleon which enters the calculation of $S_A^* S_A$. Following the technique developed in [21, 22] we can reduce the calculation of the evolution operator for the 2-body density matrix (15) to the evaluation of the S -matrix $S_{4A}(\mathbf{b}_+, \mathbf{b}_-, \mathbf{b}'_+, \mathbf{b}'_-)$ for a scattering of a fictitious 4-parton state composed of the two quark-antiquark pairs in the overall color-singlet state. Because $(T_+^a)^* = -T_-^a$, within the two-gluon exchange approximation the quarks entering the complex-conjugate S_A^* in (15) can be viewed as antiquarks, so that

$$\begin{aligned} \langle \left\{ \sum_{km} \langle 1 | S_A^*(\mathbf{b}'_+, \mathbf{b}'_-) | c_{km} \rangle \langle c_{km} | S_A(\mathbf{b}_+, \mathbf{b}_-) | 1 \rangle \right\} = \\ = \sum_{kmjl} \delta_{kl} \delta_{mj} \langle c_{km} c_{jl} | S_{4A}(\mathbf{b}'_+, \mathbf{b}'_-, \mathbf{b}_+, \mathbf{b}_-) | 11 \rangle \end{aligned} \quad (19)$$

where $S_{4A}(\mathbf{b}'_+, \mathbf{b}'_-, \mathbf{b}_+, \mathbf{b}_-)$ is an S-matrix for the propagation of the two quark-antiquark pairs in the overall singlet state. While the first $q\bar{q}$ pair is formed by the initial quark q and antiquark \bar{q} at impact parameters \mathbf{b}_+ and \mathbf{b}_- , respectively, in the second pair $q'\bar{q}'$ the quark q' propagates at an impact parameter \mathbf{b}'_- and the antiquark \bar{q}' at an impact parameter \mathbf{b}'_+ , as indicated in fig. 4. In the initial state the both quark-antiquark pairs are in color-singlet states: $|in\rangle = |11\rangle$.

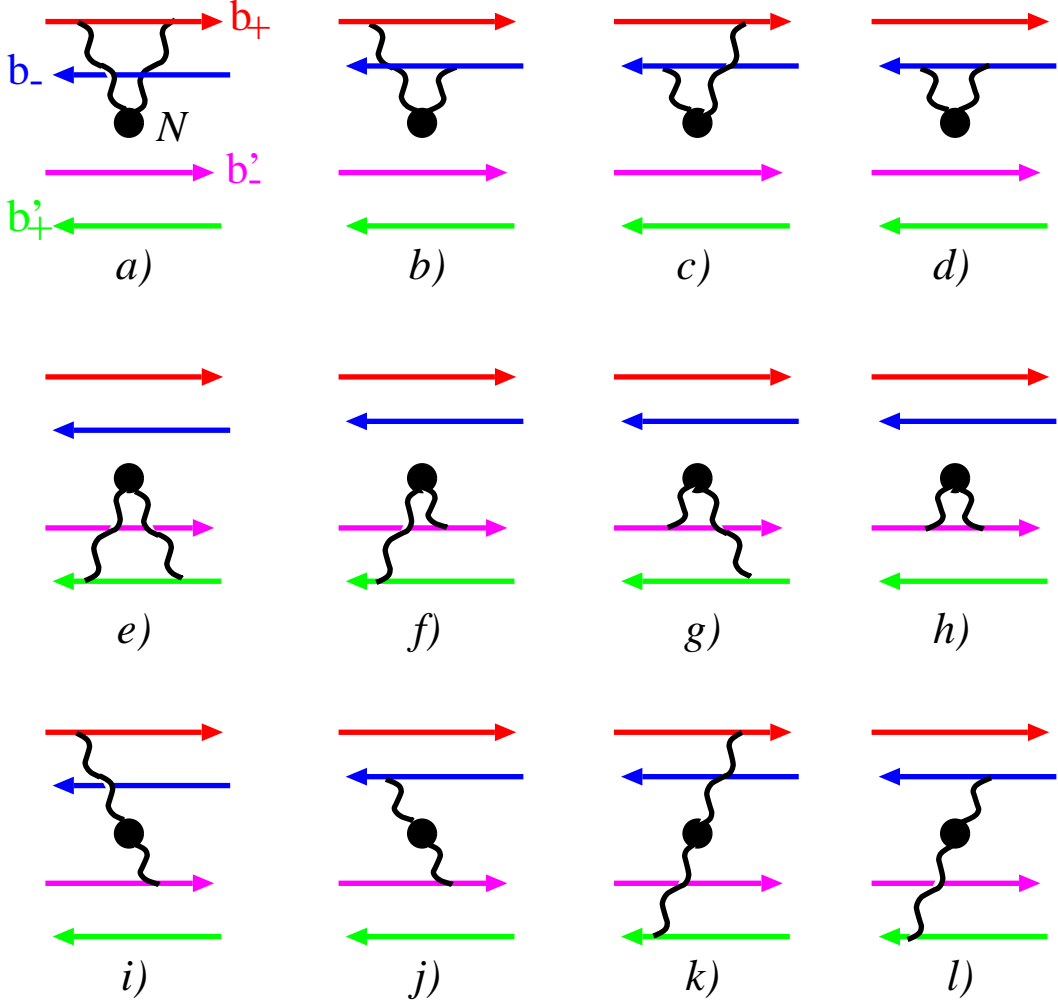


Figure 4: The p QCD diagrams for the matrix of color dipole cross section for the 4-body $(q\bar{q})(q'\bar{q}')$ state. The set 4*i*-4*l* shows only half of the diagrams for scattering with rotation of the color state of dipoles.

Let us introduce the normalized singlet-singlet and octet-octet states

$$|11\rangle = \frac{1}{N_c}(\bar{q}q)(\bar{q}'q') \quad (20)$$

$$|88\rangle = \frac{2}{\sqrt{N_c^2 - 1}}(\bar{q}T^a q)(\bar{q}'T^a q') \quad (21)$$

where N_c is the number of colors and T^a are the generators of $SU(N_c)$. Making use of the color Fiertz identity,

$$\delta_{km}\delta_{jl} = \frac{1}{N_c}\delta_l^k\delta_j^m + 2\sum_a(T^a)_l^k(T^a)_j^m \quad (22)$$

the sum over color states of the produced quark-antiquark pair can be represented as

$$\begin{aligned} \sum_{km} \langle c_{km} c_{km} | S_{4A}(\mathbf{b}'_+, \mathbf{b}'_-, \mathbf{b}_+, \mathbf{b}_-) | 11 \rangle &= \langle 11 | S_{4A}(\mathbf{b}'_+, \mathbf{b}'_-, \mathbf{b}_+, \mathbf{b}_-) | 11 \rangle \\ &+ \sqrt{N_c^2 - 1} \langle 88 | S_{4A}(\mathbf{b}'_+, \mathbf{b}'_-, \mathbf{b}_+, \mathbf{b}_-) | 11 \rangle \end{aligned} \quad (23)$$

If $\sigma_4(\mathbf{b}'_+, \mathbf{b}'_-, \mathbf{b}_+, \mathbf{b}_-)$ is the color-dipole cross section operator for the 4-body state, then the standard evaluation of the nuclear expectation value for a dilute gas nucleus gives

$$S_{4A}(\mathbf{b}'_+, \mathbf{b}'_-, \mathbf{b}_+, \mathbf{b}_-) = \exp\left\{-\frac{1}{2}\sigma_4(\mathbf{b}'_+, \mathbf{b}'_-, \mathbf{b}_+, \mathbf{b}_-)T(\mathbf{b})\right\} \quad (24)$$

where

$$T(\mathbf{b}) = \int dz n_A(z, \mathbf{b}) \quad (25)$$

is the optical thickness of a nucleus at an impact parameter $\mathbf{b} \approx \mathbf{b}_\pm, \mathbf{b}'_\pm$. In writing down (19) we employed the standard approximation of neglecting the size of color dipoles compared to a radius of heavy nucleus. The single-nucleon S -matrix (16) contains transitions from the color-singlet to the both color-singlet and color-octet $q\bar{q}$ pairs. However, only the color-singlet operators contribute to $\langle N_j | S_N^*(\mathbf{b}'_+ - \mathbf{b}_j, \mathbf{b}'_- - \mathbf{b}_j) S_N(\mathbf{b}_+ - \mathbf{b}_j, \mathbf{b}_- - \mathbf{b}_j) | N_j \rangle$, and the matrix $\sigma_4(\mathbf{b}'_+, \mathbf{b}'_-, \mathbf{b}_+, \mathbf{b}_-)$ only includes transitions between the $|11\rangle$ and $|88\rangle$ color-singlet 4-parton states, the $|18\rangle$ states are not allowed.

Performing the relevant color algebra, we find

$$\langle 11 | \sigma_4 | 11 \rangle = \sigma(\mathbf{b}_+ - \mathbf{b}_-) + \sigma(\mathbf{b}'_+ - \mathbf{b}'_-) \quad (26)$$

$$\begin{aligned} \langle 11 | \sigma_4 | 88 \rangle &= \frac{1}{\sqrt{N_c^2 - 1}} [\sigma(\mathbf{b}_- - \mathbf{b}'_-) + \sigma(\mathbf{b}_+ - \mathbf{b}'_+) \\ &\quad - \sigma(\mathbf{b}_+ - \mathbf{b}'_-) - \sigma(\mathbf{b}_- - \mathbf{b}'_+)] \end{aligned} \quad (27)$$

$$\begin{aligned} \langle 88 | \sigma_4 | 88 \rangle &= \frac{N_c^2 - 2}{N_c^2 - 1} [\sigma(\mathbf{b}_+ - \mathbf{b}'_+) + \sigma(\mathbf{b}_- - \mathbf{b}'_-)] \\ &+ \frac{2}{N_c^2 - 1} [\sigma(\mathbf{b}_+ - \mathbf{b}'_-) - \sigma(\mathbf{b}_- - \mathbf{b}'_+)] \\ &- \frac{1}{N_c^2 - 1} [\sigma(\mathbf{b}_+ - \mathbf{b}_-) + \sigma(\mathbf{b}'_+ - \mathbf{b}'_-)] \end{aligned} \quad (28)$$

The term in (14), which subtracts the contribution from processes without color excitation of the target nucleus, equals

$$\begin{aligned} \langle A | \{ \langle 1 | S_A^*(\mathbf{b}'_+, \mathbf{b}'_-) | 1 \} | A \rangle \langle A | \{ \langle 1 | S_A(\mathbf{b}_+, \mathbf{b}_-) | 1 \} | A \rangle \\ = \exp \left\{ -\frac{1}{2} [\sigma(\mathbf{b}_+ - \mathbf{b}_-) + \sigma(\mathbf{b}'_+ - \mathbf{b}'_-)] T(\mathbf{b}) \right\} \end{aligned} \quad (29)$$

Let $\Sigma_{1,2}$ be the two eigenvalues of the operator σ_4 . Then it is convenient to use the Sylvester expansion

$$\begin{aligned} \exp \left\{ -\frac{1}{2} \sigma_4 T(\mathbf{b}) \right\} = \\ \exp \left\{ -\frac{1}{2} \Sigma_1 T(\mathbf{b}) \right\} \frac{\sigma_4 - \Sigma_2}{\Sigma_1 - \Sigma_2} + \exp \left\{ -\frac{1}{2} \Sigma_2 T(\mathbf{b}) \right\} \frac{\sigma_4 - \Sigma_1}{\Sigma_2 - \Sigma_1} \end{aligned} \quad (30)$$

Evidently, in the general case the eigen-cross sections are fairly complex functions of the six possible dipoles formed by four partons. One may wonder how do the standard color-dipole Glauber-Gribov formulas [5, 2] for nuclear DIS cross sections emerge from (30)? Hence we turn first to the simpler cases of the total inelastic and single-jet inclusive cross sections. An application to (23) of the Sylvester expansion gives

$$\begin{aligned} & (\langle 11 | + \sqrt{N_c^2 - 1} \langle 88 |) \exp \left\{ -\frac{1}{2} \sigma_4 T(\mathbf{b}) \right\} | 11 \rangle \\ & - \exp \left\{ -\frac{1}{2} [\sigma(\mathbf{r}) + \sigma(\mathbf{r}')] T(\mathbf{b}) \right\} \\ & = \exp \left\{ -\frac{1}{2} \Sigma_2 T(\mathbf{b}) \right\} - \exp \left\{ -\frac{1}{2} [\sigma(\mathbf{r}) + \sigma(\mathbf{r}')] T(\mathbf{b}) \right\} \\ & + \frac{\langle 11 | \sigma_4 | 11 \rangle - \Sigma_2}{\Sigma_1 - \Sigma_2} \left\{ \exp \left[-\frac{1}{2} \Sigma_1 T(\mathbf{b}) \right] - \exp \left[-\frac{1}{2} \Sigma_2 T(\mathbf{b}) \right] \right\} \\ & + \frac{\sqrt{N_c^2 - 1} \langle 11 | \sigma_4 | 88 \rangle}{\Sigma_1 - \Sigma_2} \left\{ \exp \left[-\frac{1}{2} \Sigma_1 T(\mathbf{b}) \right] - \exp \left[-\frac{1}{2} \Sigma_2 T(\mathbf{b}) \right] \right\} \end{aligned} \quad (31)$$

4 Non-Abelian aspects of propagation of color dipoles in nuclear medium and Glauber-Gribov formalism

In order to get an insight into the impact of propagation of the color-octet $q\bar{q}$ pairs inside a nucleus let us consider first the total inelastic cross section obtained from (14) upon the integration over the transverse momenta \mathbf{p}_\pm of the quark and antiquark. Such an integration amounts to putting $\mathbf{b}_+ = \mathbf{b}'_+$ and $\mathbf{b}_- = \mathbf{b}'_-$. Then we are left with the system of two color dipoles of the same size $\mathbf{r} = \mathbf{b}_+ - \mathbf{b}_- = \mathbf{r}' = \mathbf{b}'_+ - \mathbf{b}'_-$, and the matrix of the 4-body cross sections has the eigenvalues

$$\Sigma_1 = 0, \quad (32)$$

$$\Sigma_2 = \frac{2N_c^2}{N_c^2 - 1} \sigma(\mathbf{r}) \quad (33)$$

with the eigenstates

$$|f_1\rangle = \frac{1}{N_c}(|11\rangle + \sqrt{N_c^2 - 1}|88\rangle), \quad (34)$$

$$|f_2\rangle = \frac{1}{N_c}(\sqrt{N_c^2 - 1}|11\rangle - |88\rangle). \quad (35)$$

The eigen-cross section (33) differs from $\sigma(\mathbf{r})$ for the color-singlet $q\bar{q}$ pair by the nontrivial color factor $N_c^2/(N_c^2 - 1)$. The existence of the non-attenuating 4-quark state with $\Sigma_1 = 0$ is quite obvious and corresponds to an overlap of two dipoles of the same size with neutralization of color charges.

Now notice, that the final state which enters the calculation of the genuine inelastic DIS off a nucleus, see eq. (23), is precisely the eigenstate $|f_1\rangle$. Then, even without invoking the Sylvester expansion (30), (31), the straightforward result for the inelastic cross section is

$$\begin{aligned} \sigma_{in} &= \int d^2\mathbf{r} dz |\Psi(z, \mathbf{r})|^2 \\ &\times \int d^2\mathbf{b} \left\{ N_c \langle f_1 | \exp \left[-\frac{1}{2} \sigma_4 T(\mathbf{b}) \right] |11\rangle - \exp [-\sigma(\mathbf{r}) T(\mathbf{b})] \right\} \\ &= \int d^2\mathbf{b} \langle \gamma^* | \left\{ \exp \left[-\frac{1}{2} \Sigma_1 T(\mathbf{b}) \right] - \exp [-\sigma(\mathbf{r}) T(\mathbf{b})] \right\} | \gamma^* \rangle \\ &= \int d^2\mathbf{b} \langle \gamma^* | \{1 - \exp [-\sigma(\mathbf{r}) T(\mathbf{b})]\} | \gamma^* \rangle \end{aligned} \quad (36)$$

what is precisely the Glauber-Gribov formula [2] in which no trace of a propagation inside a nucleus of the eigenstate (35) with the eigen-cross section (33) is left.

When the final state $q\bar{q}$ is produced in the color-singlet state, the net flow of color between the $q\bar{q}$ pair and color-excited debris of the target nucleus is zero. Which suggests that a rapidity gap may survive upon the hadronization, although whether a rapidity gap in genuine inelastic events with color-singlet $q\bar{q}$ production is stable against higher order correction or not remains an interesting open issue. Here we proceed under the assumption that the rapidity gap survives and the production of the color-singlet and color-octet $q\bar{q}$ pairs can be separated. Although the debris of the target nucleus have a zero net color charge, the color-excited debris of nucleons are spatially separated by a distance of the order of the nuclear radius. The formation of color strings between the color centers would lead to a total excitation energy of the order of 1 GeV times $A^{1/3}$, so that such a rapidity-gap events would look like a double diffraction with multiple production of mesons in the nucleus fragmentation region (for the theoretical discussion of conventional mechanisms of diffraction excitation of nuclei in proton-nucleus collisions see [23], the experimental observation has been reported in [24]). As such it is distinguishable from quasielastic diffractive DIS followed by excitation and breakup of the target nucleus without production of secondary particles.

Making use of the Sylvester expansion (30)-(31), and the eigenstates (34),(35), one readily obtains

$$\sigma_{in}(A^*(q\bar{q})_1) =$$

$$\int d^2\mathbf{b} \langle \gamma^* | \left\{ (1 - \exp[-\sigma(\mathbf{r})T(\mathbf{b})]) - \frac{N_c^2 - 1}{N_c^2} (1 - \exp\left[-\frac{1}{2}\Sigma_2 T(\mathbf{b})\right]) \right\} |\gamma^* \rangle \quad (37)$$

and

$$\sigma_{in}(A^*(q\bar{q})_8) = \frac{N_c^2 - 1}{N_c^2} \int d^2\mathbf{b} \langle \gamma^* | \left\{ 1 - \exp\left[-\frac{1}{2}\Sigma_2 T(\mathbf{b})\right] \right\} |\gamma^* \rangle. \quad (38)$$

In the latter case the nontrivial eigen-cross section Σ_2 enters explicitly.

Several features of the result (37) are noteworthy. First, the color neutralization of the $q\bar{q}$ pair after the first inelastic interaction requires at least one secondary inelastic interaction. Indeed, an expansion of the integrand starts with the term quadratic in the optical thickness:

$$\begin{aligned} & \left\{ (1 - \exp[-\sigma(\mathbf{r})T(\mathbf{b})]) - \frac{N_c^2 - 1}{N_c^2} (1 - \exp\left[-\frac{1}{2}\Sigma_2 T(\mathbf{b})\right]) \right\} \\ &= \frac{\sigma^2(\mathbf{r})T^2(\mathbf{b})}{2(N_c^2 - 1)} + \dots \end{aligned} \quad (39)$$

Second, in the large- N_c limit the color octet state tends to oscillate in color remaining in the octet state. This is clearly seen from (39). Third, in the limit of an opaque nucleus

$$\sigma_{in}(A^*(q\bar{q})_1) = \frac{1}{N_c^2} \int d^2\mathbf{b} \langle \gamma^* | \{ 1 - \exp[-\sigma(\mathbf{r})T(\mathbf{b})] \} |\gamma^* \rangle = \frac{1}{N_c^2} \sigma_{in} \quad (40)$$

and remains a constant fraction of DIS in contrast to the quasielastic diffractive DIS or inelastic diffractive excitation of a nucleus, the cross sections of which vanish for an opaque nucleus [2, 23].

The result (38) shows how the non-Abelian nature of the propagation of color dipoles inside a nucleus which manifests itself via the eigen-cross section (33) distinct from $\sigma(\mathbf{r})$ reveals itself in the total cross section of inelastic DIS with excitation of dijets in the color-octet state.

An analysis of the single-parton, alias the single-jet, inclusive cross section is quite similar. In this case we integrate over the momentum \mathbf{p}_- of the antiquark jet, so that $\mathbf{b}'_- = \mathbf{b}_-$. The matrix σ_4 has the eigenvalues

$$\Sigma_1 = \sigma(\mathbf{r} - \mathbf{r}') \quad (41)$$

$$\Sigma_2 = \frac{N_c^2}{N_c^2 - 1} [\sigma(\mathbf{r}) + \sigma(\mathbf{r}')] - \frac{1}{N_c^2 - 1} \sigma(\mathbf{r} - \mathbf{r}') \quad (42)$$

with exactly the same eigenstates $|f_1\rangle$ and $|f_2\rangle$ as given by eqs. (34),(35). Again, the cross section of genuine inelastic DIS corresponds to projection onto the eigenstate $|f_1\rangle$, so that [8]

$$\frac{d\sigma_{in}}{d^2\mathbf{b} d^2\mathbf{p} dz} = \frac{1}{(2\pi)^2} \int d^2\mathbf{r}' d^2\mathbf{r} \exp[i\mathbf{p}(\mathbf{r}' - \mathbf{r})] \Psi^*(\mathbf{r}') \Psi(\mathbf{r})$$

$$\begin{aligned}
& \times \left\{ \exp\left[-\frac{1}{2}\Sigma_1 T(\mathbf{b})\right] - \exp\left[-\frac{1}{2}[\sigma(\mathbf{r}) + \sigma(\mathbf{r}')]T(\mathbf{b})\right] \right\} \\
& = \frac{1}{(2\pi)^2} \int d^2\mathbf{r}' d^2\mathbf{r} \exp[i\mathbf{p}(\mathbf{r}' - \mathbf{r})] \Psi^*(\mathbf{r}') \Psi(\mathbf{r}) \\
& \times \left\{ \exp\left[-\frac{1}{2}\sigma(\mathbf{r} - \mathbf{r}')T(\mathbf{b})\right] - \exp\left[-\frac{1}{2}[\sigma(\mathbf{r}) + \sigma(\mathbf{r}')]T(\mathbf{b})\right] \right\}. \quad (43)
\end{aligned}$$

5 The Pomeron-Splitting Mechanism for Diffractive Hard Dijets and Weizsäcker-Williams glue of nuclei

At QCD parton level diffraction dissociation of photons and hadrons is modeled by excitation of $q\bar{q}$, $q\bar{q}g$, ... Fock states which are lifted on their mass shell through the t -channel exchange of a QCD Pomeron with the target hadron. The color singlet two-gluon structure of the Pomeron gives rise to the two distinct forward $q\bar{q}$ dijet production subprocesses: The first one, of fig. 3e (also fig. 5a), is a counterpart of the classic Landau-Pomeranchuk [25, 26, 27] mechanism of diffraction dissociation of deuterons into the proton-neutron continuum and can be dubbed the splitting of the beam particle into the dijet, because the transverse momentum \mathbf{k} of jets comes from the intrinsic transverse momentum of quarks and antiquarks in the beam particle. Specific of QCD is the mechanism of fig. 3f (also fig. 5b) where jets receive a transverse momentum from gluons in the Pomeron. In an extension of the early work [9], in [10] it was shown that the second mechanism dominates at a sufficiently large \mathbf{k} and in this regime diffractive amplitudes are proportional to the differential (unintegrated) gluon structure function $\mathcal{F}(x, \mathbf{k}^2) = \partial G(x, \mathbf{k}^2) / \partial \log \mathbf{k}^2$. Correspondingly, this mechanism has been dubbed splitting of the Pomeron into dijets. In diffractive DIS the Pomeron splitting dominates at $k \gg Q$, whereas the somewhat modified Landau et al. mechanism dominates at $k \lesssim Q$.

Motivated by the recent data from the E791 Fermilab experiment [28], here we discuss peculiarities of the Pomeron splitting mechanism on an example of diffractive excitation of pions into dijets on free nucleon and nuclear targets. In a slight adaption of the results of [9, 10] one should replace the pointlike $\gamma^* q\bar{q}$ vertex $eA_\mu \bar{\Psi} \gamma_\mu \Psi$ by the non-pointlike $\pi q\bar{q}$ vertex $i\Gamma(M^2) \bar{\Psi} \gamma_5 \Psi$. Here $M^2 = (\mathbf{k}^2 + m_f^2)/z(1-z)$ is the invariant mass squared of the dijet system, the pion momentum is shared by the jets in the partitioning $z, 1-z$. The explicit form of the spinor vertex reads

$$\bar{\Psi}_\lambda(\mathbf{k}) \gamma_5 \Psi_{\bar{\lambda}}(-\mathbf{k}) = \frac{\lambda}{\sqrt{z(1-z)}} [m_f \delta_{\lambda-\bar{\lambda}} - \sqrt{2} \mathbf{k} \cdot \mathbf{e}_{-\lambda} \delta_{\lambda\bar{\lambda}}], \quad (44)$$

where m_f is the quark mass, λ and $\bar{\lambda}$ are the quark and antiquark helicities and $\mathbf{e}_\lambda = -(\lambda \mathbf{e}_x + i \mathbf{e}_y)/\sqrt{2}$. The two helicity amplitudes $\Phi_0(z, \mathbf{k}, \Delta)$ for $\lambda + \bar{\lambda} = 0$ and $\Phi_1(z, \mathbf{k}, \Delta)$ for $\lambda + \bar{\lambda} = \pm 1$, can be cast in the form (we concentrate on the forward limit, $\Delta = 0$)

$$\Phi_0(z, \mathbf{k}) = \alpha_S(\mathbf{k}^2) \sigma_0 \left[\int d^2\kappa m_f \psi_\pi(z, \mathbf{k}) f(\kappa) - \int d^2\kappa m_f \psi_\pi(z, \kappa) f(\mathbf{k} - \kappa) \right], \quad (45)$$

and Φ_1 is obtained from the substitution $m_f\psi(z, \mathbf{k}) \rightarrow \mathbf{k}\psi(z, \mathbf{k})$. The radial wave function of the $q\bar{q}$ Fock state of the pion is related to the $\pi q\bar{q}$ vertex function as

$$\psi_\pi(z, \mathbf{k}) = \frac{N_c}{4\pi^3 z(1-z)} \frac{\Gamma_\pi(M^2)}{(M^2 - m_\pi^2)} \quad (46)$$

and is normalized to the $\pi \rightarrow \mu\nu$ decay constant $F_\pi = 131$ MeV through

$$F_\pi = \int d^2\mathbf{k} dz m_f \psi_\pi(z, \mathbf{k}) = F_\pi \int_0^1 dz \phi_\pi(z), \quad (47)$$

where $\phi_\pi(z)$ is the pion distribution amplitude [29]. Finally, our normalization of helicity amplitudes is such, that the differential cross section of forward dijet production equals

$$\frac{d\sigma_D}{dz d\mathbf{k}^2 d\Delta^2} \Big|_{\Delta=0} = \frac{\pi^3}{24} \left\{ |\Phi_0|^2 + |\Phi_1|^2 \right\}. \quad (48)$$

We turn to the discussion of the asymptotics for large jet momenta \mathbf{k} . The first term in eq.(45) comes from the Landau et al. pion splitting mechanism of fig. 5a, whereas the second one is the contribution from the Pomeron splitting of fig. 5b. Because $\psi_\pi \otimes f$ is a convolution of nonoscillating functions, it is necessarily a broader function than $\psi_\pi(z, \mathbf{k})$ and thus will take over if only \mathbf{k} is large enough. For the quantitative estimate, we remind the reader, that for $x \sim 10^{-2}$ relevant to the kinematics of E791, the large- \mathbf{k} behavior of $f(\mathbf{k})$ is well described by the inverse power law $f(\mathbf{k}) \propto k^{-2\delta}$ with an exponent $\delta \sim 2.15$ [30]. Clearly, $f(\mathbf{k})$ decreases much slower than $\psi(z, \mathbf{k})$, and hence the asymptotics of the convolution integral is controlled by the asymptotics of $f(\mathbf{k})$:

$$\int d^2\kappa m_f \psi_\pi(z, \kappa) f(\mathbf{k} - \kappa) \approx f(\mathbf{k}) \int d^2\kappa m_f \psi_\pi(z, \kappa) = f(\mathbf{k}) \phi_\pi(z) F_\pi, \quad (49)$$

which shows that in this regime the dijet momentum comes entirely from the momentum of gluons in the Pomeron. Furthermore, in the same regime diffraction into dijets probes the pion distribution amplitude $\phi_\pi(z)$.

Now we notice that in the color dipole representation

$$\Phi_0(z, \mathbf{k}) = \int d^2\mathbf{r} e^{-i\mathbf{k}\mathbf{r}} \sigma(\mathbf{r}) m_f \Psi_\pi(z, \mathbf{r}), \quad (50)$$

and the nuclear amplitude is readily obtained [5] by substituting in eq.(50)

$$\sigma(\mathbf{r}) \rightarrow \sigma_A(\mathbf{r}) = 2 \int d^2\mathbf{b} \left\{ 1 - \exp\left[-\frac{1}{2}\sigma(\mathbf{r})T_A(\mathbf{b})\right] \right\} \quad (51)$$

Typical nuclear double scattering diagrams of figs. 5c-5e can conveniently be classified as nuclear shadowing of the pion splitting (fig. 5c), nuclear shadowing of single Pomeron splitting (fig. 5d) and double Pomeron splitting (fig. 5e) contributions. The j Pomeron splitting is due to diagrams, in which j of the Pomerons exchanged between the color

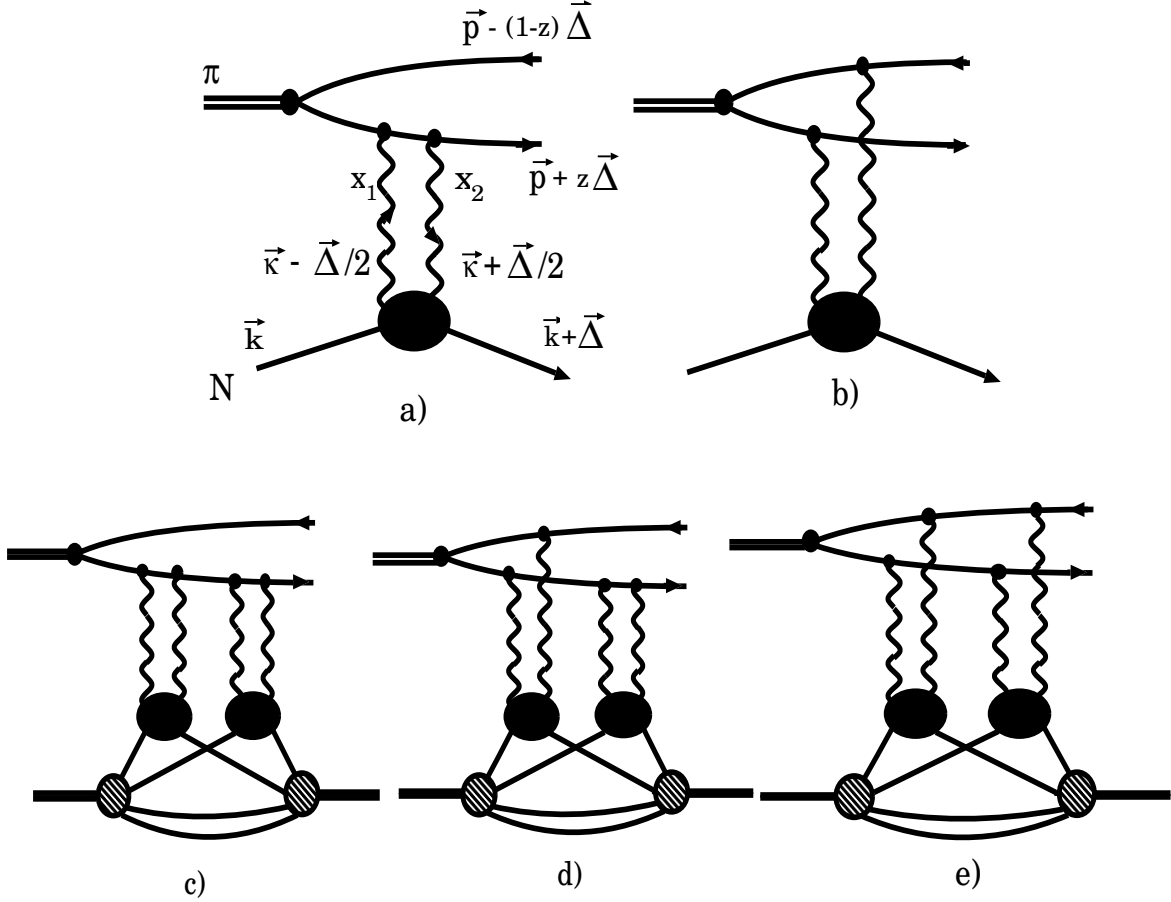


Figure 5: Sample Feynman diagrams for diffractive dijet excitation in πN collisions [diagrams 5a), 5b)] and typical rescattering corrections to the nuclear coherent amplitude [diagrams 5c), 5d), 5e)].

dipole and the nucleus couple with one gluon to the quark and with one gluon to the antiquark and involve the j -fold convolutions of the unintegrated gluon distribution

$$f^{(j)}(\boldsymbol{\kappa}) = \int \prod_{i=1}^j d^2 \boldsymbol{\kappa}_i f(\boldsymbol{\kappa}_i) \delta(\boldsymbol{\kappa} - \sum_{i=1}^j \boldsymbol{\kappa}_i). \quad (52)$$

Now we can invoke the NSS representation for the nuclear attenuation factor [11, 8]

$$\begin{aligned} \exp \left[-\frac{1}{2} \sigma(\mathbf{s}) T(\mathbf{b}) \right] &= \exp [-\nu_A(\mathbf{b})] \exp \left[\nu_A(\mathbf{b}) \int d^2 \boldsymbol{\kappa} f(\boldsymbol{\kappa}) \exp(i \boldsymbol{\kappa} \mathbf{s}) \right] \\ &= \exp [-\nu_A(\mathbf{b})] \sum_{j=0}^{\infty} \frac{\nu_A^j(\mathbf{b})}{j!} \int d^2 \boldsymbol{\kappa} f^{(j)}(\boldsymbol{\kappa}) \exp(i \boldsymbol{\kappa} \mathbf{s}) \\ &= \int d^2 \boldsymbol{\kappa} \Phi(\nu_A(\mathbf{b}), \boldsymbol{\kappa}) \exp(i \boldsymbol{\kappa} \mathbf{s}) \end{aligned} \quad (53)$$

where

$$\Phi(\nu_A(\mathbf{b}), \boldsymbol{\kappa}) = \exp(-\nu_A(\mathbf{b})) f^{(0)}(\boldsymbol{\kappa}) + \phi_{WW}(\mathbf{b}, \boldsymbol{\kappa}), \quad (54)$$

$$\nu_A(\mathbf{b}) = \frac{1}{2} \alpha_S(r) \sigma_0 T(\mathbf{b}) \quad (55)$$

and it is understood that

$$f^{(0)}(\boldsymbol{\kappa}) = \delta(\boldsymbol{\kappa}). \quad (56)$$

Then the multiple-Pomeron splitting expansion for nuclear diffractive amplitude takes the form

$$\begin{aligned} \Phi_0^{(A)}(z, \mathbf{k}, \boldsymbol{\Delta}) = 2m_f \int d^2 \mathbf{b} e^{-i \mathbf{b} \boldsymbol{\Delta}} & \left\{ \Psi_\pi(z, \mathbf{k}) \left[1 - \exp \left(-\frac{\sigma_{eff}(\mathbf{k}^2)}{2} T_A(\mathbf{b}) \right) \right] \right. \\ & \left. - \sum_{j \geq 1} \int d^2 \boldsymbol{\kappa} \Psi_\pi(z, \boldsymbol{\kappa}) \phi_{WW}(\mathbf{k} - \boldsymbol{\kappa}) \right\}. \end{aligned} \quad (57)$$

A comparison with (45) suggests that $\phi_{WW}(\boldsymbol{\kappa})$ can be identified with the unintegrated nuclear Weizsäcker-Williams glue per unit area in the impact parameter plane [8]. In (54) we kept an explicit dependence on the optical thickness of the nucleus.

6 Nuclear dilution and broadening of the unintegrated Weizsäcker-Williams glue of nuclei

On the one hand, according to [11, 8] the multiple convolutions $f^{(j)}(\boldsymbol{\kappa})$ have a meaning of the collective unintegrated gluon structure function of j nucleons at the same impact parameter the Weizsäcker-Williams gluon fields of which overlap spatially in the Lorentz contracted nucleus. On the other hand, these convolutions of can also be viewed as a random walk in which $f(\boldsymbol{\kappa})$ describes the single walk distribution. To the lowest order in pQCD, the large $\boldsymbol{\kappa}^2$ behavior is

$$f(\boldsymbol{\kappa}) \propto \frac{\alpha_S(\boldsymbol{\kappa}^2)}{(\boldsymbol{\kappa}^2)^2} \quad (58)$$

The QCD evolution effects enhance $f(\boldsymbol{\kappa})$ at large $\boldsymbol{\kappa}^2$, the smaller is x the stronger is an enhancement. Because $f(\boldsymbol{\kappa})$ decreases very slowly, we encounter a manifestly non-Gaussian random walk. For instance, as was argued in [11], a j -fold walk to large $\boldsymbol{\kappa}^2$ is realized by one large walk, $\boldsymbol{\kappa}_1^2 \sim \boldsymbol{\kappa}^2$, accompanied by $(j-1)$ small walks. We simply cite here the main result [11]

$$f^{(j)}(\boldsymbol{\kappa}) = j \cdot f(\boldsymbol{\kappa}) \left[1 + \frac{4\pi^2(j-1)\gamma^2}{N_c \sigma_0 \boldsymbol{\kappa}^2} \cdot G(\boldsymbol{\kappa}^2) \right] \quad (59)$$

where $G(\kappa^2)$ is the conventional integrated gluon structure function and γ is an exponent of the large- κ^2 asymptotics of the differential glue in the proton,

$$f(\kappa) \propto \frac{1}{(\kappa^2)^\gamma} \quad (60)$$

Then the hard tail of unintegrated nuclear glue per bound nucleon can be calculated parameter free:

$$f_{WW}(\kappa) = f(\kappa) \left[1 + \frac{2C_A\pi^2\gamma^2\alpha_S(r)T(\mathbf{b})}{C_F N_c \kappa^2} G(\kappa^2) \right] \quad (61)$$

In the hard regime the differential nuclear glue is not shadowed, furthermore, because of the manifestly positive-valued and model-independent nuclear higher twist correction it exhibits nuclear antishadowing property [11].

Now we present the arguments in favor of the soft- κ behavior

$$f^{(j)}(\kappa) \approx \frac{1}{\pi} \frac{Q_j^2}{(\kappa^2 + Q_j^2)^2} = \frac{1}{Q_j^2} \chi\left(\frac{\kappa^2}{Q_j^2}\right) \quad (62)$$

with the width

$$Q_j^2 \sim j Q_0^2 \quad (63)$$

In an evolution of $f^{(j)}(\kappa)$ with j at moderate κ^2 ,

$$f^{(j+1)}(\kappa^2) = \int d^2\mathbf{k} f(\mathbf{k}^2) f^{(j)}((\kappa - \mathbf{k})^2) \quad (64)$$

the function $f(\mathbf{k}^2)$ is a steep one compared to a smooth and broad $f^{(j)}((\kappa - \mathbf{k})^2)$, so that we can expand

$$\begin{aligned} f^{(j)}((\kappa - \mathbf{k})^2) &= \\ f^{(j)}(\kappa^2) &+ \frac{df^{(j)}(\kappa^2)}{d\kappa^2} [\mathbf{k}^2 - 2\kappa\mathbf{k}] + \frac{1}{2} \frac{d^2 f^{(j)}(\kappa^2)}{(d\kappa^2)^2} 4(\kappa\mathbf{k})^2 \\ \implies f^{(j)}(\kappa^2) &+ \left[\frac{df^{(j)}(\kappa^2)}{d\kappa^2} + \kappa^2 \frac{d^2 f^{(j)}(\kappa^2)}{(d\kappa^2)^2} \right] \mathbf{k}^2 \\ = f^{(j)}(\kappa^2) &+ \frac{d}{d\kappa^2} \left[\kappa^2 \frac{df^{(j)}(\kappa^2)}{d\kappa^2} \right] \mathbf{k}^2 \end{aligned} \quad (65)$$

Here \implies indicates an azimuthal averaging. Our expansion was valid for $\mathbf{k}^2 \lesssim Q_j^2$, hence

$$\begin{aligned} f^{(j+1)}(\kappa^2) &= f^{(j)}(\kappa^2) + \frac{d}{d\kappa^2} \left[\kappa^2 \frac{df^{(j)}(\kappa^2)}{d\kappa^2} \right] \int^{Q_j^2} d^2\mathbf{k} f(\mathbf{k}^2) \mathbf{k}^2 \\ &= f^{(j)}(\kappa^2) + g(j) \frac{d}{d\kappa^2} \left[\kappa^2 \frac{df^{(j)}(\kappa^2)}{d\kappa^2} \right] \end{aligned} \quad (66)$$

where

$$g(j) = \int^{Q_j^2} d^2\mathbf{k} \mathbf{k}^2 f(\mathbf{k}^2) = \frac{4\pi^2}{N_c \sigma_0} G(Q_j^2) \quad (67)$$

is a smooth function of j .

For small κ^2 the recurrence relation amounts to

$$\frac{Q_{j+1}^2 - Q_j^2}{Q_{j+1}^2 Q_j^2} = -\frac{1}{Q_j^4} \frac{\chi'(0)}{\chi(0)} g(j) \quad (68)$$

which, for large j , reduces to a differential equation

$$\frac{dQ_j^2}{dj} = -\frac{\chi'(0)}{\chi(0)} g(j) \quad (69)$$

with the solution

$$Q_j^2 = -\frac{\chi'(0)}{\chi(0)} \int^j dj' g(j') \approx -j g(j) \frac{\chi'(0)}{\chi(0)} \approx j Q_0^2. \quad (70)$$

The expansion (65) holds up to the terms $\propto \kappa^2$ and its differentiation at $\kappa^2 = 0$ gives a similar constraint on the j -dependence of Q_j^2 . The soft parameters Q_0^2 and σ_0 are related to the integrated glue of the proton in the soft region,

$$Q_0^2 \sigma_0 \sim \frac{2\pi^2}{N_c} G_{soft}, \quad G_{soft} \sim 1. \quad (71)$$

We conclude by the observation that when extended to $\kappa^2 \gtrsim Q_j^2$, the parameterization (62), (63) has the behavior $j Q_0^2 / (\kappa^2)^2$ which nicely matches the j -dependence of the leading twist term in the hard asymptotics (61).

An approximation (62), (63) is corroborated by the numerical results for the j -dependence of convolutions calculated for the unintegrated gluon structure function of the proton from ref. [30], see fig. 6.

For heavy nuclei the dominant contribution to $\phi_{WW}(\kappa)$ comes from $j \approx \nu_A(\mathbf{b})$, and the gross features of the WW nuclear glue in the soft region are well reproduced by

$$\phi_{WW}(\kappa) \approx \frac{1}{\pi} \frac{Q_A^2}{(\kappa^2 + Q_A^2)^2}, \quad (72)$$

where the saturation scale $Q_A^2 = \nu_A(\mathbf{b}) Q_0^2 \propto A^{1/3}$.

Notice a strong nuclear dilution of soft WW glue,

$$\phi_{WW}(\kappa) \propto 1/Q_A^2 \propto A^{-1/3} \quad (73)$$

which must be contrasted to the A -dependence of hard glue, cf. (59), (61),

$$\phi_{WW}(\kappa) = \nu_A(\mathbf{b}) f_{WW}(\kappa) \propto A^{1/3} \times (1 + A^{1/3} \times (HT) + \dots). \quad (74)$$

Take the platinum target, $A = 192$. The numerical estimates show that for $(q\bar{q})$ color dipoles in the average DIS on this target $\nu_A \approx 4$ and $Q_{3A}^2 \approx 0.8 \text{ GeV}^2$. For the $q\bar{q}g$ Fock

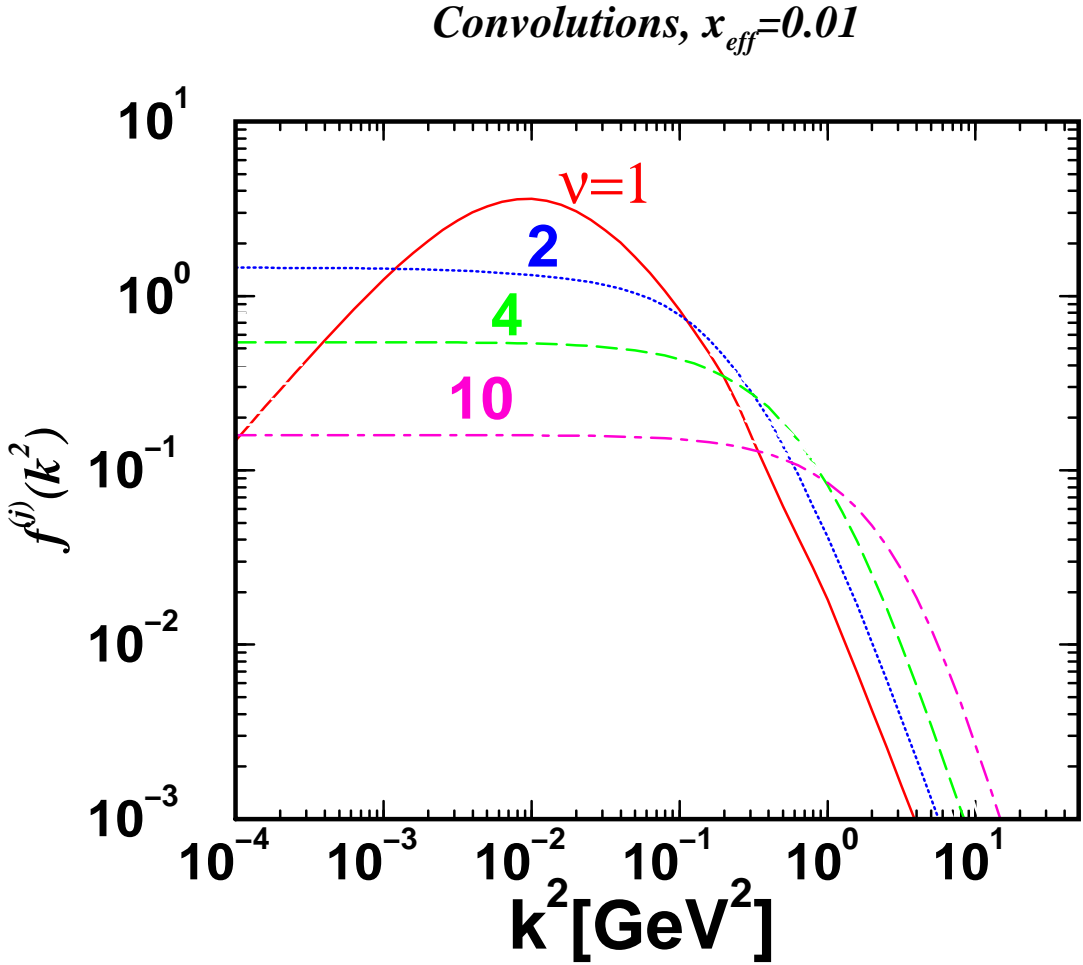


Figure 6: The dilution for soft momenta and broadening for hard momenta of the multiple convolutions $f^{(j)}(\kappa)$.

states of the photon, which behave predominantly like the dipole made of the two octet color charges, the saturation scale is larger by the factor $C_A/C_F = 9/4$,

$$Q_{8A}^2 = \frac{C_A}{C_F} Q_{3A}^2. \quad (75)$$

The numerical estimates for the the average DIS on the Pt target give $Q_{8A}^2 \approx 2.2 \text{ GeV}^2$.

7 Back to the hard diffraction of pions: the interpretation of the E791 data

The detailed numerical analysis for the kinematics of the E791 experiment is found in [11]. In fig. 7 we only show the numerical result of the \mathbf{k} dependence of the dijet cross

section with the (unnormalized) data from E791. We note in passing that the region of jet momenta $k \lesssim 1.5$ GeV is contaminated by diffractive excitation of heavy mesons a_1, π' , etc, and in this region the use of plane wave parton model formulas is not warranted. Our calculations for smaller k only serve to give an idea on how the pion splitting dominates at small k and how the pomeron splitting mechanism takes over beyond the dip in Φ_0^2 and Φ_1^2 . The latter is a higher twist term. In the pomeron splitting dominance region of $k > 1.5$ GeV we find good agreement with the experimentally observed \mathbf{k} -dependence. We wish to warn the reader however, that for the kinematics of E791 the dijet cross section receives a huge contribution from the antishadowing nuclear higher twist correction [11].

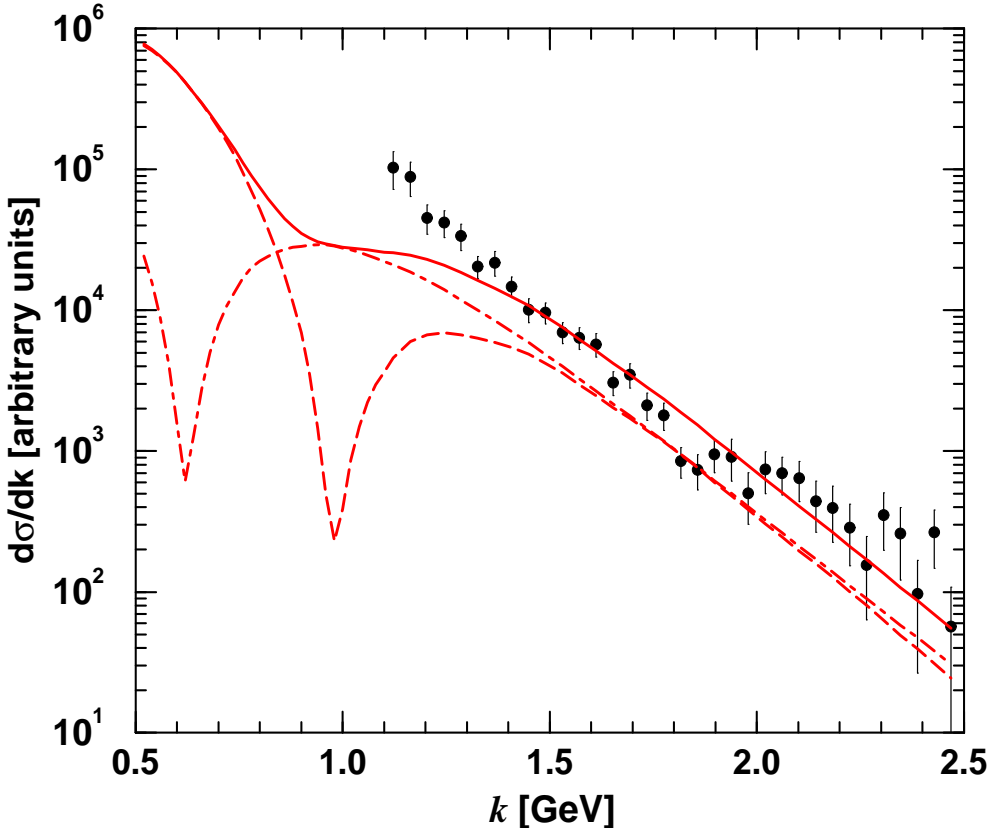


Figure 7: The E791 data [28] for the differential diffractive dijet cross section $d\sigma/dk$ for the ^{196}Pt target with the theoretical calculations. The data are not normalized. The dash-dotted line shows the contribution of the helicity amplitude $\Phi_0^{(A)}$, the dashed line is the contribution from $\Phi_1^{(A)}$. The solid line is the total result.

The effect of antishadowing nuclear higher twist correction is especially obvious in fig. 8, where we show the exponent α of the A -dependence $\sigma \sim A^\alpha$. In the impulse approximation

$$\sigma \propto \frac{A^2}{R_A^2} \sim A^{4/3} \quad (76)$$

If the exponent α is defined from a comparison of the cross sections for the carbon and

platinum targets, then the impulse approximation gives $\alpha \approx 1.44$. For hard dijets our antishadowing effect predicts a substantial excess of α over the impulse approximation value.

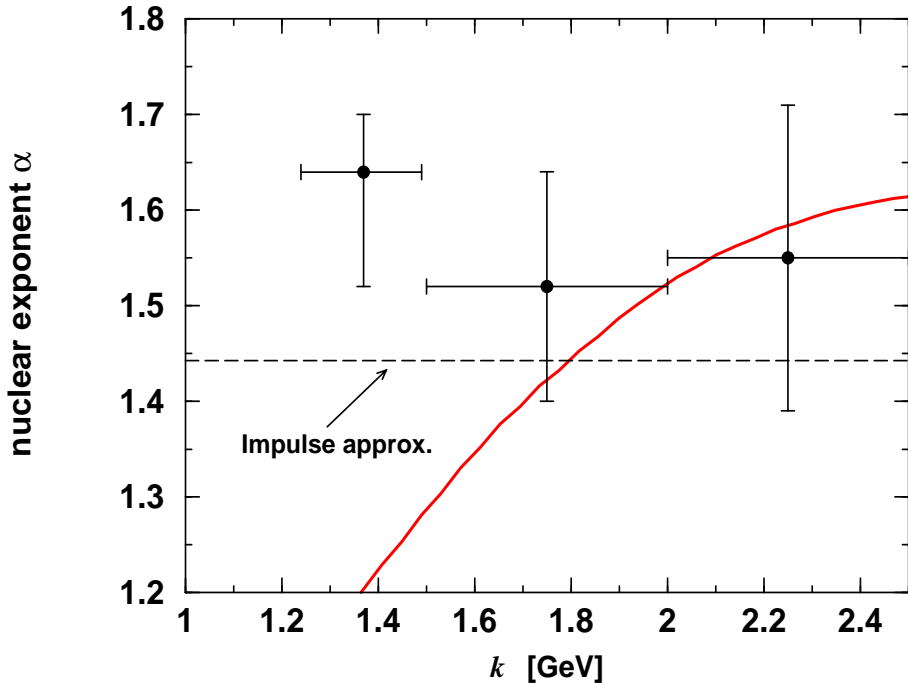


Figure 8: The E791 data [28] for the exponent of the A dependence of the jet cross section vs. the theoretical calculations shown by the solid curve.

The NSS dominance of the pomeron-splitting contribution for hard dijets has fully been confirmed by the collinear factorization NLO order analysis of Chernyak et al. [31] and Braun et al. [32]. The NLO correction to the NSS amplitude is found to be proportional to the asymptotic distribution amplitude and numerically quite substantial, so that the experimental data by E791 [28] can not distinguish between the asymptotic and double-humped distribution amplitudes. According to NSS [11] realistic model distributions do not differ much from the asymptotic one, though. To our view, the only caveat in the interpretation of the NLO results is that the issue of partial reabsorption of these corrections into the evolution/renormalization of the pion distribution amplitude still needs further scrutiny. Anyway, there emerges a consistent pattern of diffraction of pions into hard dijets and in view of these findings the claims by Frankfurt et al. [33] that the diffractive amplitude is proportional to the integrated gluon structure function of the target must be regarded null and void. (Hopefully, some day the E791 collaboration shall report on the interpretation of their results within the correct formalism.)

8 Nuclear partons in the saturation regime

Here we apply the results of sections 4 and 5 to the calculation of FS single-parton (jet) spectrum for nuclear targets. On the one hand, making use of the NSS representation, the total nuclear photoabsorption cross section (51) can be cast in the form

$$\sigma_A = \int d^2\mathbf{b} \int dz \int \frac{d^2\mathbf{p}}{(2\pi)^2} \int d^2\boldsymbol{\kappa} \phi_{WW}(\boldsymbol{\kappa}) |\langle \gamma^* | \mathbf{p} \rangle - \langle \gamma^* | \mathbf{p} - \boldsymbol{\kappa} \rangle|^2 \quad (77)$$

which has a profound semblance to (8) and one is tempted to take the differential form of (77) as a definition of the IS sea quark density in a nucleus (hereafter we consider one flavour and take e_f^2 the factor out of the photon's wave function and cross sections):

$$\frac{d\bar{q}_{IS}}{d^2\mathbf{b} d^2\mathbf{p}} = \frac{1}{2} \cdot \frac{Q^2}{4\pi^2\alpha_{em}} \cdot \frac{d\sigma_A}{d^2\mathbf{b} d^2\mathbf{p}}. \quad (78)$$

In terms of the WW nuclear glue, all intranuclear multiple-scattering diagrams of fig. 3g sum up to precisely the same four diagrams fig. 3a-3d as in DIS off free nucleons. Furthermore, one can argue that the small- x evolution of the so-defined IS nuclear sea is similar to that for a free nucleon sea. Although \mathbf{p} emerges here just as a formal Fourier parameter, we shall demonstrate that it can be identified with the momentum of the observed final state antiquark.

On the other hand, making use of the NSS representation, after some algebra one finds

$$\begin{aligned} & \exp[-\frac{1}{2}\sigma(\mathbf{r} - \mathbf{r}')T(\mathbf{b})] - \exp[-\frac{1}{2}[\sigma(\mathbf{r}) + \sigma(\mathbf{r}')]T(\mathbf{b})] = \\ & \int d^2\boldsymbol{\kappa} \phi_{WW}(\boldsymbol{\kappa}) \{ (\exp[i\boldsymbol{\kappa}(\mathbf{r} - \mathbf{r}')] - 1) + (1 - \exp[i\boldsymbol{\kappa}\mathbf{r}]) + (1 - \exp[i\boldsymbol{\kappa}'\mathbf{r}']) \} \\ & - \int d^2\boldsymbol{\kappa} \phi_{WW}(\boldsymbol{\kappa}) (1 - \exp[i\boldsymbol{\kappa}\mathbf{r}]) \int d^2\boldsymbol{\kappa}' \phi_{WW}(\boldsymbol{\kappa}') (1 - \exp[i\boldsymbol{\kappa}'\mathbf{r}']) \end{aligned} \quad (79)$$

so that the single-quark spectrum (43) takes the form

$$\begin{aligned} \frac{d\sigma_{in}}{d^2\mathbf{b} d^2\mathbf{p} dz} &= \frac{1}{(2\pi)^2} \left\{ \int d^2\boldsymbol{\kappa} \phi_{WW}(\boldsymbol{\kappa}) |\langle \gamma^* | \mathbf{p} \rangle - \langle \gamma^* | \mathbf{p} - \boldsymbol{\kappa} \rangle|^2 \right. \\ &\quad \left. - \left| \int d^2\boldsymbol{\kappa} \phi_{WW}(\boldsymbol{\kappa}) (\langle \gamma^* | \mathbf{p} \rangle - \langle \gamma^* | \mathbf{p} - \boldsymbol{\kappa} \rangle) \right|^2 \right\} \end{aligned} \quad (80)$$

$$\frac{d\sigma_D}{d^2\mathbf{b} d^2\mathbf{p} dz} = \frac{1}{(2\pi)^2} \left| \int d^2\boldsymbol{\kappa} \phi_{WW}(\boldsymbol{\kappa}) (\langle \gamma^* | \mathbf{p} \rangle - \langle \gamma^* | \mathbf{p} - \boldsymbol{\kappa} \rangle) \right|^2. \quad (81)$$

Putting the inelastic and diffractive components of the FS quark spectrum together, we evidently find the FS parton density which exactly coincides with the IS parton density (78) such that \mathbf{p} is indeed the transverse momentum of the FS sea quark. The interpretation of this finding is not trivial, though.

Consider first the domain of $\mathbf{p}^2 \lesssim Q^2 \lesssim Q_A^2$ such that the nucleus is opaque for all color dipoles in the photon. Hereafter we assume that the saturation scale Q_A^2 is so large that \mathbf{p}^2, Q^2 are in the pQCD domain and neglect the quark masses. In this regime the

nuclear counterparts of the crossing diagrams of figs. 3b,3d,3f can be neglected. Then, in the classification of [11], diffraction will be dominated by the contribution from the Landau-Pomeranchuk diagram of fig. 3e with the result

$$\begin{aligned} \frac{d\bar{q}_{FS}}{d^2\mathbf{b}d^2\mathbf{p}}\Big|_D &= \frac{1}{2} \cdot \frac{Q^2}{4\pi^2\alpha_{em}} \cdot \frac{d\sigma_D}{d^2\mathbf{b}d^2\mathbf{p}} \\ &\approx \frac{1}{2} \cdot \frac{Q^2}{4\pi^2\alpha_{em}} \cdot \int dz \left| \int d^2\kappa \phi_{WW}(\kappa) \right|^2 |\langle \gamma^* | \mathbf{p} \rangle|^2 \\ &\approx \frac{N_c}{4\pi^4}. \end{aligned} \quad (82)$$

Up to now we specified neither the wave function of the photon nor the spin nor the color representation of charged partons, only the last result in (82) makes an explicit use of the conventional spin- $\frac{1}{2}$ partons. Remarkably, diffractive DIS measures the momentum distribution of quarks and antiquarks in the $q\bar{q}$ Fock state of the photon. We emphasize that this result, typical of the Landau-Pomeranchuk mechanism, is a completely generic one and would hold for any beam particle such that its coupling to hard colored partons is weak. In contrast to diffraction off free nucleons [9, 10, 34], diffraction off opaque nuclei is dominated by the anti-collinear splitting of hard gluons into soft sea quarks, $\kappa^2 \gg \mathbf{p}^2$. Precisely for this reason one finds the saturated FS quark density, because the nuclear dilution of the WW glue is compensated for by the expanding plateau. The result (82) has no counterpart in DIS off free nucleons because diffractive DIS off free nucleons is negligibly small even at HERA, $\eta_D \lesssim 6\text{-}10\%$ [14].

The related analysis of the FS quark density for truly inelastic DIS in the same domain of $\mathbf{p}^2 \lesssim Q^2 \lesssim Q_A^2$ gives

$$\begin{aligned} \frac{d\bar{q}_{FS}}{d^2\mathbf{b}d^2\mathbf{p}}\Big|_{in} &= \frac{1}{2} \cdot \frac{Q^2}{4\pi^2\alpha_{em}} \cdot \int dz \int d^2\kappa \phi_{WW}(\kappa) |\langle \gamma^* | \mathbf{p} - \kappa \rangle|^2 \\ &= \frac{Q^2}{8\pi^2\alpha_{em}} \phi_{WW}(0) \int^{Q^2} d^2\kappa \int dz |\langle \gamma^* | \kappa \rangle|^2 \\ &= \frac{N_c}{4\pi^4} \cdot \frac{Q^2}{Q_A^2} \cdot \theta(Q_A^2 - \mathbf{p}^2). \end{aligned} \quad (83)$$

It describes final states with color excitation of a nucleus, but as a function of the photon wave function and nuclear WW gluon distribution it is completely different from (8) for free nucleons. The θ -function simply indicates that the plateau for inelastic DIS extends up to $\mathbf{p}^2 \lesssim Q_A^2$. For $Q^2 \ll Q_A^2$ the inelastic plateau contributes little to the transverse momentum distribution of soft quarks, $\mathbf{p}^2 \lesssim Q^2$, but the inelastic plateau extends way beyond Q^2 and its integral contribution to the spectrum of FS quarks is exactly equal to that from diffractive DIS. Such a two-plateau structure of the FS quark spectrum is a new finding and has not been considered before.

Now notice, that in the opacity regime the diffractive FS parton density coincides with the contribution $\propto |\langle \gamma^* | \mathbf{p} \rangle|^2$ to the IS sea parton density from the spectator diagram of fig. 3a, whereas the FS parton density for truly inelastic DIS coincides with the contribution

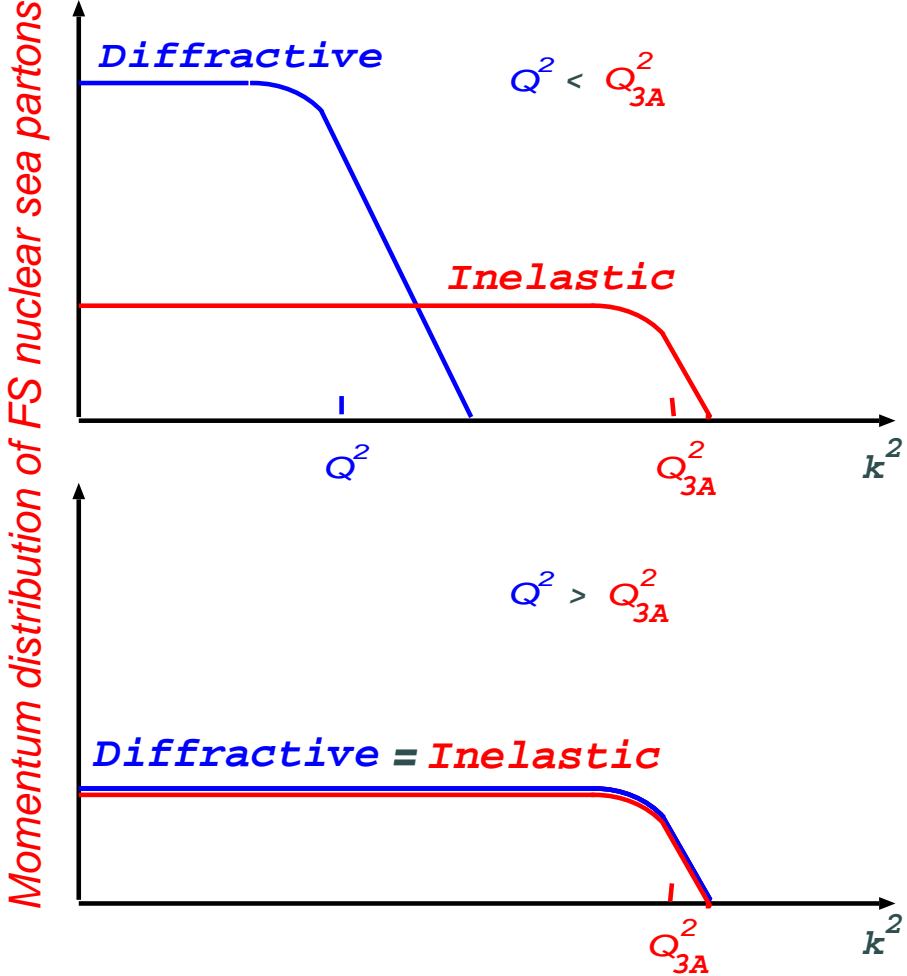


Figure 9: The two-plateau structure of the momentum distribution of FS quarks: (i) $Q^2 \lesssim Q_{3A}^2$: The inelastic plateau is much broader than the diffractive one. (ii) $Q^2 \gtrsim Q_{3A}^2$: inelastic plateau is identical to diffractive one.

to IS sea partons from the diagram of fig. 3c. In this regime the contribution from the crossing diagrams of figs. 3b,d is negligibly small.

Our results (82) and (83), especially nuclear broadening and unusually strong Q^2 dependence of the FS/IS parton density from truly inelastic DIS, demonstrate clearly a distinction between diffractive and inelastic DIS. Our considerations can readily be extended to the spectrum of soft quarks, $\mathbf{p}^2 \lesssim Q_A^2$, in hard photons, $Q^2 \gtrsim Q_A^2$. In this case the result (82) for diffractive DIS is retained, whereas in the numerator of the result (83) for truly inelastic DIS one must substitute $Q^2 \rightarrow Q_A^2$, so that in this case $dq_{FS}|_D \approx dq_{FS}|_{in}$ and $dq_{IS} \approx 2dq_{FS}|_D$. The evolution of soft nuclear sea, $\mathbf{p}^2 \lesssim Q_A^2$, is entirely driven by an anti-collinear splitting of the NSS-defined WW nuclear glue into the sea partons.

The early discussion of the FS quark density in the saturation regime is due to Mueller [35]. Mueller focused on $Q^2 \gg Q_A^2$ and discussed neither a distinction between diffractive

and truly inelastic DIS nor a Q^2 dependence and broadening (83) for truly inelastic DIS at $Q^2 \lesssim Q_A^2$.

A comparison with the IS nuclear parton densities which evolve from the NSS-defined WW nuclear glue shows an exact equality of the FS and IS parton densities. The plateau-like saturated nuclear quark density is suggestive of the Fermi statistics, but our principal point that for any projectile which interacts weakly with colored partons the saturated density measures the momentum distribution in the $q\bar{q}, gg, \dots$ Fock state of the projectile disproves the Fermi-statistics interpretation. The spin and color multiplet of colored partons the photon couples to is completely irrelevant, what only counts is an opacity of heavy nuclei. The anti-collinear splitting of WW nuclear glue into soft sea partons is a noteworthy feature of the both diffractive DIS and IS sea parton distributions. The emergence of a saturated density of IS sea partons from the nuclear-diluted WW glue is due to the nuclear broadening of the plateau (83). Because the predominance of diffraction is a very special feature of DIS [2], one must be careful with applying the IS parton densities to, for instance, nuclear collisions, in which diffraction wouldn't be of any significance.

9 Signals of saturation in exclusive diffractive DIS

A flat \mathbf{p}^2 distribution of forward q, \bar{q} jets in truly inelastic DIS in the saturation regime, see eq. (83), must be contrasted to the standard DGLAP spectrum,

$$\frac{d\bar{q}}{d^2\mathbf{p}} = \frac{2\alpha_S(\mathbf{p}^2)G(\mathbf{p}^2)}{3\pi\mathbf{p}^2}, \quad (84)$$

for the free nucleon target.

In the diffractive DIS the signal of saturation is much more dramatic: a flat \mathbf{p}^2 distribution of forward q, \bar{q} jets in diffractive DIS in the saturation regime, see eq. (82), must be contrasted to the spectrum

$$\frac{d\sigma_D}{d^2\mathbf{p}} \propto \frac{G^2(\mathbf{p}^2)}{(\mathbf{p}^2)^2} \quad (85)$$

in diffractive DIS off the free nucleon target [9, 10, 34]. Recall that it is \mathbf{p}^2 which serves as a hard scale for diffractive dijets unless \mathbf{p}^2 is so large that the pomeron splitting mechanism takes over [10, 34].

In the general case one must compare the saturation scale Q_A to the relevant hard scale for the specific diffractive process. For instance, in the exclusive diffractive DIS, i.e., the vector meson production, the hard scale for the proton target equals [36]

$$\bar{Q}^2 \approx \frac{1}{4}(Q^2 + m_V^2) \quad (86)$$

and the transverse cross section has been predicted to behave as [36]

$$\sigma_T \propto \left[\frac{G(x, \bar{Q}^2)}{\bar{Q}^4} \right]^2 \quad (87)$$

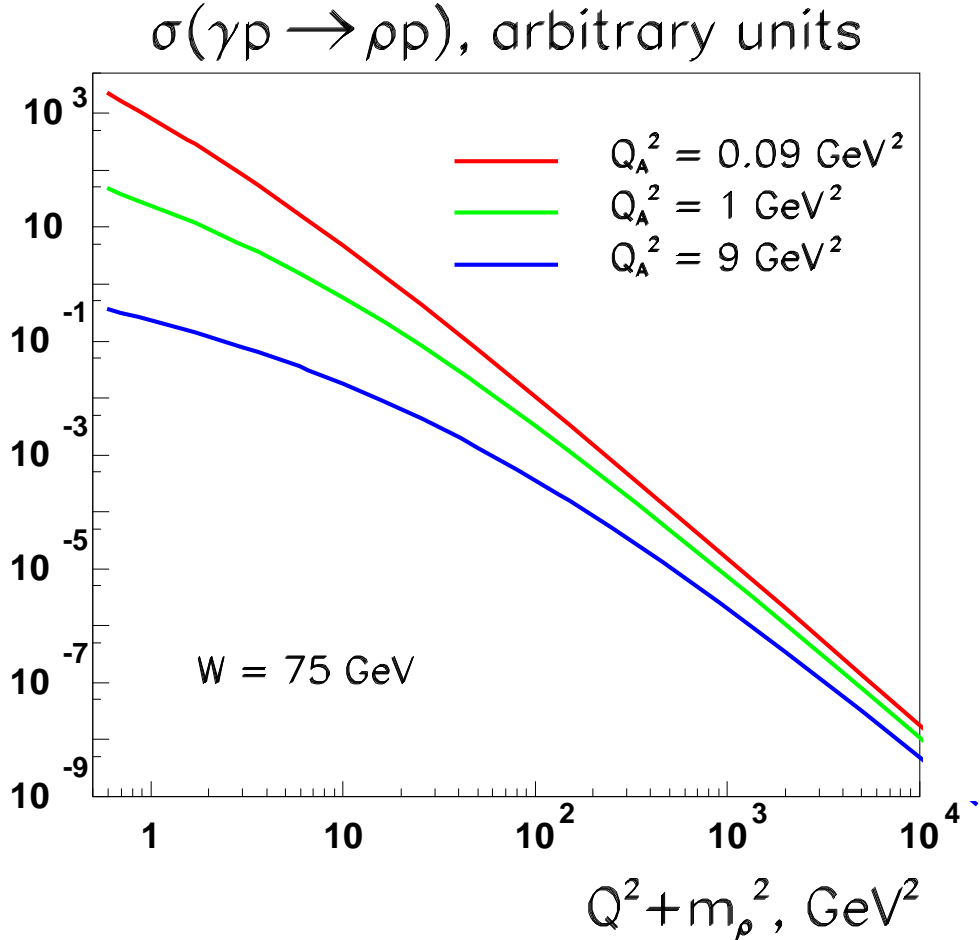


Figure 10: The modification of the $(Q^2 + m_V^2)$ dependence of diffractive ρ production from a free nucleon target (small saturation scale Q_A^2) to a nucleus (large Q_A^2) with the change of the saturation scale Q_A^2 .

At $\bar{Q}^2 > Q_A^2$ the same would hold for nuclei too, but in the opposite case of $\bar{Q}^2 < Q_A^2$ the \bar{Q}^2 -dependence is predicted to change to

$$\sigma_T \propto \left[\frac{G(x, \bar{Q}^2)}{Q_A^2 \bar{Q}^2} \right]^2 \quad (88)$$

The numerical results shown in Fig. 10 give an idea on how the $(Q^2 + m_V^2)$ dependence of exclusive diffraction into the vector mesons changes from the free nucleon to nuclear target with the increasing saturation scale.

As shown in [37], there is a duality correspondence between the $(Q^2 + m_V^2)$ dependence of exclusive production of vector mesons and the mass spectrum of diffractive DIS into small-mass continuum states, i.e, at large values, $\beta \rightarrow 1$, of the diffractive Bjorken variable

$$\beta = \frac{Q^2}{M^2 + Q^2}. \quad (89)$$

Specifically, for diffractive DIS off free nucleons the transverse diffractive structure function has the large- β behavior [34]

$$F_D \propto (1 - \beta)^2, \quad (90)$$

whereas in diffractive DIS off nuclei in the saturation regime we predict

$$F_D \propto (1 - \beta). \quad (91)$$

10 Jet-jet (de)correlation in DIS off nuclear targets: hard jets

The diagonalization of the 2×2 matrix σ_4 derived in section 3 is a straightforward task, so that technically eqs. (14) and (26)-(30) allow a direct calculation of the jet-jet inclusive cross section in terms of the color dipole cross section $\sigma(\mathbf{r})$. The practical evaluation of the 6-fold Fourier transform is not a trivial task, though, and analytical evaluations are called upon. Here we focus on production of forward hard jets with the momenta $\mathbf{p}_\pm^2 \gtrsim Q_A^2$, where Q_A is the saturation scale. Such hard jets are produced from interactions with the target nucleus of small color dipoles in the incident photon such that diffractive nuclear attenuation effects can be neglected. In this case useful and intuitively transparent analytic results for the jet-jet (de)correlation can be obtained.

Before proceeding to this approximation, it is convenient to introduce the average impact parameter

$$\mathbf{b} = \frac{1}{4}(\mathbf{b}_+ + \mathbf{b}'_+ + \mathbf{b}_- + \mathbf{b}'_-), \quad (92)$$

(one should not confuse \mathbf{b} with the center of gravity of color dipoles where the impact parameters \mathbf{b}_\pm and \mathbf{b}'_\pm must be weighted with z_\pm) and

$$\mathbf{s} = \mathbf{b}_+ - \mathbf{b}'_+, \quad (93)$$

for the variable conjugate to the decorrelation momentum, in terms of which

$$\mathbf{b}_+ - \mathbf{b}'_- = \mathbf{s} + \mathbf{r}', \quad (94)$$

$$\mathbf{b}_- - \mathbf{b}'_+ = \mathbf{s} - \mathbf{r}, \quad (95)$$

$$\mathbf{b}_- - \mathbf{b}'_- = \mathbf{s} - \mathbf{r} + \mathbf{r}'. \quad (96)$$

We also reproduce here the matrix elements of σ_4 in this basis:

$$\langle 11 | \sigma_4 | 11 \rangle = \sigma(\mathbf{r}) + \sigma(\mathbf{r}') \quad (97)$$

$$\langle 11 | \sigma_4 | 88 \rangle = \frac{1}{\sqrt{N_c^2 - 1}} [\sigma(\mathbf{s}) - \sigma(\mathbf{s} + \mathbf{r}') - \sigma(\mathbf{s} - \mathbf{r}) + \sigma(\mathbf{s} - \mathbf{r} + \mathbf{r}')] \quad (98)$$

$$\begin{aligned}
\langle 88 | \sigma_4 | 88 \rangle &= \frac{N_c^2 - 2}{N_c^2 - 1} [\sigma(\mathbf{s}) + \sigma(\mathbf{s} - \mathbf{r} + \mathbf{r}')] \\
&+ \frac{2}{N_c^2 - 1} [\sigma(\mathbf{s} + \mathbf{r}') - \sigma(\mathbf{s} - \mathbf{r})] \\
&- \frac{1}{N_c^2 - 1} [\sigma(\mathbf{r}) + \sigma(\mathbf{r}')]
\end{aligned} \tag{99}$$

Hard jets correspond to $|\mathbf{r}|, |\mathbf{r}'| \ll |\mathbf{s}|$. Then the two eigenvalues are

$$\Sigma_2 = \langle 11 | \sigma_4 | 11 \rangle \approx 0 \tag{100}$$

and

$$\Sigma_1 = \langle 88 | \sigma_4 | 88 \rangle \approx 2 \frac{N_c^2 - 2}{N_c^2 - 1} \sigma(\mathbf{s}) = 2\lambda_c \sigma(\mathbf{s}) \tag{101}$$

where $\lambda_c = (N_c^2 - 2)/(N_c^2 - 1)$. Because of (100) only the second term, $\propto \langle 11 | \sigma_4 | 88 \rangle$, must be kept in the Sylvester expansion (31). It is convenient to define the nuclear distortion factor

$$D_A(\mathbf{s}, \mathbf{r}, \mathbf{r}') = \frac{2}{(\Sigma_2 - \Sigma_1)T(\mathbf{b})} \left\{ \exp \left[-\frac{1}{2}\Sigma_1 T(\mathbf{b}) \right] - \exp \left[-\frac{1}{2}\Sigma_2 T(\mathbf{b}) \right] \right\} \tag{102}$$

such that to the leading order in nuclear thickness, i.e., in the impulse approximation, $D_A(\mathbf{s}, \mathbf{r}, \mathbf{r}') = 1$. Then, the impulse approximation cross section per unit area in the impact parameter plane takes the form (we expose the relevant steps in some detail)

$$\begin{aligned}
\frac{d\sigma_{IA}}{d^2\mathbf{b} dz d^2\mathbf{p}_+ d^2\mathbf{p}_-} &= \frac{-1}{2(2\pi)^4} \int d^2\mathbf{s} d^2\mathbf{r} d^2\mathbf{r}' \\
&\times \exp[-i(\mathbf{p}_+ + \mathbf{p}_-)\mathbf{s} + i\mathbf{p}_-(\mathbf{r}' - \mathbf{r})] \Psi^*(\mathbf{r}') \Psi(\mathbf{r}) \\
&\times T(\mathbf{b}) \sqrt{N_c^2 - 1} \langle 11 | \sigma_4 | 88 \rangle D_A(\mathbf{s}, \mathbf{r}, \mathbf{r}', \mathbf{b}) \\
&= \frac{1}{2(2\pi)^4} T(\mathbf{b}) \int d^2\mathbf{s} d^2\mathbf{r} d^2\mathbf{r}' \exp[-i(\mathbf{p}_+ + \mathbf{p}_-)\mathbf{s} + \mathbf{p}_-(\mathbf{r}' - \mathbf{r})] \\
&\times \Psi^*(\mathbf{r}') \Psi(\mathbf{r}) [\sigma(\mathbf{s}) - \sigma(\mathbf{s} + \mathbf{r}') - \sigma(\mathbf{s} - \mathbf{r}) + \sigma(\mathbf{s} - \mathbf{r} + \mathbf{r}')] \tag{103}
\end{aligned}$$

Here we employ the integral representation (4):

$$\begin{aligned}
&[\sigma(\mathbf{s}) - \sigma(\mathbf{s} + \mathbf{r}') - \sigma(\mathbf{s} - \mathbf{r}) + \sigma(\mathbf{s} - \mathbf{r} + \mathbf{r}')] \\
&= \alpha_S \sigma_0 \int d^2\Delta f(\Delta) \exp[i\Delta\mathbf{s}] \{1 - \exp[i\Delta\mathbf{r}']\} \{1 - \exp[-i\Delta\mathbf{r}]\} \tag{104}
\end{aligned}$$

which leads to the Impulse Approximation result

$$\begin{aligned}
\frac{d\sigma_{IA}}{d^2\mathbf{b} dz d^2\mathbf{p}_+ d^2\mathbf{p}_-} &= \frac{1}{2(2\pi)^4} \alpha_S \sigma_0 T(\mathbf{b}) \int d^2\mathbf{s} d^2\mathbf{r} d^2\mathbf{r}' d^2\Delta f(\Delta) \\
&\times \exp[i(\Delta - \mathbf{p}_+ - \mathbf{p}_-)\mathbf{s}] \exp[i\mathbf{p}_-(\mathbf{r}' - \mathbf{r})] \\
&\times \Psi^*(\mathbf{r}') \{1 - \exp[i\Delta\mathbf{r}']\} \Psi(\mathbf{r}) \{1 - \exp[-i\Delta\mathbf{r}]\} \tag{105}
\end{aligned}$$

The $d^2\mathbf{s}$ integration entails $\Delta = \mathbf{p}_+ - \mathbf{p}_-$, the remaining Fourier transforms are straightforward and give precisely (12) times $T(\mathbf{b})$:

$$\frac{d\sigma_{IA}}{d^2\mathbf{b} dz d^2\mathbf{p}_+ d^2\Delta} = T(\mathbf{b}) \frac{d\sigma_N}{d^2\mathbf{b} dz d^2\mathbf{p}_+ d^2\Delta} \quad (106)$$

The nuclear distortion factor takes a simple form

$$\begin{aligned} D_A(\mathbf{s}, \mathbf{b}) &= \frac{\exp\left[-\frac{1}{2}\Sigma_1 T(\mathbf{b})\right] - 1}{\frac{1}{2}\Sigma_1 T(\mathbf{b})} = \int_0^1 d\beta \exp\left[-\frac{1}{2}\beta\Sigma_1 T(\mathbf{b})\right] \\ &= \int_0^1 d\beta \int d^2\kappa \Phi(2\beta\lambda_c\nu_A(\mathbf{b}), \kappa) \exp(i\kappa\mathbf{s}) \end{aligned} \quad (107)$$

The introduction of this distortion factor into (105) is straightforward and gives our central result for the hard jet-jet inclusive cross section:

$$\frac{d\sigma_{in}}{d^2\mathbf{b} dz d^2\mathbf{p}_+ d^2\Delta} = T(\mathbf{b}) \int_0^1 d\beta \int d^2\kappa \Phi(2\beta\lambda_c\nu_A(\mathbf{b}), \Delta - \kappa) \frac{d\sigma_N}{dz d^2\mathbf{p}_+ d^2\kappa}. \quad (108)$$

It has a probabilistic form of a convolution of the differential cross section on a free nucleon target with $\Phi(2\beta\lambda_c\nu_A(\mathbf{b}), \kappa)$. Here β has a meaning of the fraction of the nuclear thickness which the $(q\bar{q})$ pair propagates in the color octet state.

In the practical calculations one can use an explicit expansion

$$\int_0^1 d\beta \Phi(2\beta\lambda_c\nu_A(\mathbf{b}), \Delta) = \sum_{j=0}^{\infty} \frac{1}{j!} \frac{\gamma(j+1, 2\beta\lambda_c\nu_A(\mathbf{b}))}{2\beta\lambda_c\nu_A(\mathbf{b})} f^{(j)}(\Delta), \quad (109)$$

where $\gamma(j, x)$ is an incomplete Gamma-function. For heavy nuclei the dominant contribution comes from $j \sim \nu_A$. Neglecting the small departure of λ_c from unity, for a heavy nucleus we can approximate

$$\begin{aligned} \int_0^1 d\beta \Phi(2\beta\lambda_c\nu_A(\mathbf{b}), \Delta) &\approx \Phi(\lambda_c\nu_A(\mathbf{b}), \Delta) \\ &\approx \Phi(\nu_A(\mathbf{b}), \Delta) \approx \frac{1}{\pi} \frac{Q_A^2}{(\Delta^2 + Q_A^2)^2} \end{aligned} \quad (110)$$

and evaluate the gross features of a jet-jet decorrelation analytically. First, notice that $f(\kappa)$ which enters the free nucleon cross section (12) is a steep function of κ compared to a broad distribution (110). Then,

$$\begin{aligned} \frac{d\sigma_{in}}{d^2\mathbf{b} dz d^2\mathbf{p}_+ d^2\Delta} &\approx T(\mathbf{b}) \frac{Q_A^2}{\pi(\Delta^2 + Q_A^2)^2} \int d^2\kappa \frac{d\sigma_N}{dz d^2\mathbf{p}_+ d^2\kappa} \\ &\approx \frac{1}{2} T(\mathbf{b}) e_f^2 \alpha_{em} \alpha_S(\mathbf{p}_+^2) [z^2 + (1-z)^2] G(\Delta^2 + Q_A^2) \\ &\times \frac{Q_A^2}{\pi(\Delta^2 + Q_A^2)^2} \frac{\varepsilon^4 + (\mathbf{p}_+^2)^2}{(\varepsilon^2 + \mathbf{p}_+^2)^4}, \end{aligned} \quad (111)$$

where the integrated gluon structure function of the nucleon enters at the factorization scale $\approx (\Delta^2 + Q_A^2)$. Neglecting the scaling violations in $G(\Delta^2 + Q_A^2)$, we can evaluate expectation value $\langle \Delta_\perp^2 \rangle$ subject to the condition $\Delta^2 \lesssim \mathbf{p}_+^2$ as

$$\langle \Delta_\perp^2 \rangle \approx \frac{Q_A^2}{2} \left(\frac{Q_A^2 + \mathbf{p}_+^2}{\mathbf{p}_+^2} \log \frac{Q_A^2 + \mathbf{p}_+^2}{Q_A^2} - 1 \right) \quad (112)$$

The differential out-of-plane momentum distribution can be evaluated as

$$\frac{d\sigma}{d\Delta_\perp} \approx \frac{1}{2} \frac{Q_A^2}{(Q_A^2 + \Delta_\perp^2)^{3/2}} \quad (113)$$

which shows that the probability to observe the away jet at $\Delta_\perp \sim 0$ disappears $\propto 1/Q_A \propto 1/\sqrt{\nu_A}$.

The probabilistic character of our result (108) can be understood as follows. Hard jets originate from small color dipoles. Their interaction with gluons of the target nucleus is suppressed by screening of color charges of the quark and antiquark in the color-singlet $q\bar{q}$ state which is manifest from the small cross section for a free nucleon target, see eqs. (12), (13). The first inelastic interaction inside a nucleus converts the $q\bar{q}$ pair into the color-octet state. The color charges of the quark and antiquark are no longer screened and rescatterings of the quark and antiquark in the color field of intranuclear nucleons are uncorrelated. Consequently, the broadening of the momentum distribution with nuclear thickness follows the probabilistic picture.

11 Disappearance of jet-jet correlation in DIS off nuclear targets: minijets below the saturation scale

In the above discussion of the single particle spectrum we discovered that the sea quarks evolve via the anticolinear, anti-DGLAP splitting of gluons into sea, when the transverse momentum of the parent gluons is larger than the momentum of the sea quarks [8], which suggests strongly a complete azimuthal decorrelation of forward jets with the transverse momenta below the saturation scale, $\mathbf{p}_\perp^2 \lesssim Q_A^2$. Our numerical results reported in section 6 suggest that for the realistic nuclei Q_A^2 does not exceed several GeV^2 , hence this regime is a somewhat academic one. Still, let us assume that Q_A is so large that jets with $\mathbf{p}_\perp^2 \lesssim Q_A^2$ are measurable.

Upon the slight generalization of (107) the distortion factor admits a representation

$$D_A(\mathbf{s}, \mathbf{r}, \mathbf{r}', \mathbf{b}) = \int_0^1 d\beta \exp \left\{ -\frac{1}{2} [\beta \Sigma_1 + (1 - \beta) \Sigma_2] T(\mathbf{b}) \right\}. \quad (114)$$

It is still too complex if one is after the exact eigenvalues $\Sigma_{1,2}$, however, it simplifies greatly if one invokes the large- N_c approximation, in which case

$$\Sigma_2 = \langle 11 | \sigma_4 | 11 \rangle = \sigma(\mathbf{r}) + \sigma(\mathbf{r}') \quad (115)$$

and

$$\Sigma_1 = \sigma(\mathbf{s}) + \sigma(\mathbf{s} + \mathbf{r}' - \mathbf{r}). \quad (116)$$

Because in the large- N_c approximation $\Sigma_2 = \langle 11|\sigma_4|11\rangle = \sigma(\mathbf{r}) + \sigma(\mathbf{r}')$, the first two terms in the Sylvester expansion (31) do vanish and only the last term will contribute to the jet-jet inclusive cross section. In the large- N_c approximation there is only one transition from the color-singlet to the color-octet state, once in the color octet state the $q\bar{q}$ only oscillates in the color space. Then the different exponentials in the resulting distortion factor

$$\begin{aligned} D_A(\mathbf{s}, \mathbf{r}, \mathbf{r}', \mathbf{b}) &= \int_0^1 d\beta \exp \left\{ -\frac{1}{2}\beta[\sigma(\mathbf{s}) + \sigma(\mathbf{s} + \mathbf{r}' - \mathbf{r})]T(\mathbf{b}) \right\} \\ &\quad \times \exp \left\{ -\frac{1}{2}(1 - \beta)[\sigma(\mathbf{r}) + \sigma(\mathbf{r}')]T(\mathbf{b}) \right\} \end{aligned} \quad (117)$$

admit a simple interpretation: The last two exponential factors describe the intranuclear distortion of the incoming color-singlet ($q\bar{q}$) dipole state, whereas the former two factors describe the distortion of the outgoing color-octet dipole states.

A straightforward generalization of (107) gives

$$\begin{aligned} D_A(\mathbf{s}, \mathbf{r}, \mathbf{r}', \mathbf{b}) &= \int_0^1 d\beta \int d^2\kappa_1 \Phi((1 - \beta)\nu_A(\mathbf{b}), \kappa_1) \exp(-i\kappa_1 \mathbf{r}) \\ &\quad \times \int d^2\kappa_2 \Phi((1 - \beta)\nu_A(\mathbf{b}), \kappa_2) \exp(i\kappa_2 \mathbf{r}) \\ &\quad \times \int d^2\kappa_3 \Phi(\beta\nu_A(\mathbf{b}), \kappa_3) \exp[i\kappa_3(\mathbf{s} + \mathbf{r}' - \mathbf{r})] \\ &\quad \times \int d^2\kappa_4 \Phi(\beta\nu_A(\mathbf{b}), \kappa_4) \exp(i\kappa_4 \mathbf{r}) \end{aligned} \quad (118)$$

and the jet-jet inclusive cross section takes the form

$$\begin{aligned} \frac{d\sigma_{in}}{d^2\mathbf{b} dz d\mathbf{p}_- d\Delta} &= \frac{1}{2(2\pi)^2} \alpha_S \sigma_0 T(\mathbf{b}) \int_0^1 d\beta \int d^2\kappa_1 d^2\kappa_2 d^2\kappa_3 d^2\kappa f(\kappa) \\ &\quad \times \Phi((1 - \beta)\nu_A(\mathbf{b}), \kappa_1) \Phi((1 - \beta)\nu_A(\mathbf{b}), \kappa_2) \\ &\quad \times \Phi(\beta\nu_A(\mathbf{b}), \kappa_3) \Phi(\beta\nu_A(\mathbf{b}), \Delta - \kappa_3 - \kappa) \\ &\quad \times \{\Psi(-\mathbf{p}_- + \kappa_2 + \kappa_3) - \Psi(-\mathbf{p}_- + \kappa_2 + \kappa_3 + \kappa)\}^* \\ &\quad \times \{\Psi(-\mathbf{p}_- + \kappa_1 + \kappa_3) - \Psi(-\mathbf{p}_- + \kappa_1 + \kappa_3 + \kappa)\} \end{aligned} \quad (119)$$

It is uniquely calculable in terms of the NSS-defined WW glue of the nucleus.

Now consider the limiting case of minijets with the transverse momentum below the saturation scale, $|\mathbf{p}_-|, |\Delta| \lesssim Q_A$. Notice, that $|\kappa_i| \sim Q_A$, so that one can neglect \mathbf{p}_- in the photon's wave functions and the decorrelation momentum Δ in the argument of $\Phi(\beta\nu_A(\mathbf{b}), \Delta - \kappa_3 - \kappa)$. The gross features of the product of the photon's wave functions which enters the integrand of (119), after the averaging over κ_1 and κ_2 can be well approximated by

$$\begin{aligned} &\langle \{\Psi(-\mathbf{p}_- + \kappa_2 + \kappa_3) - \Psi(-\mathbf{p}_- + \kappa_2 + \kappa_3 + \kappa)\}^* \\ &\quad \{\Psi(-\mathbf{p}_- + \kappa_1 + \kappa_3) - \Psi(-\mathbf{p}_- + \kappa_1 + \kappa_3 + \kappa)\} \rangle_{\kappa_{1,2}} \\ &\implies |\Psi(\kappa_3) - \Psi(\kappa_3 + \kappa)|^2 \end{aligned} \quad (120)$$

The principal point is that the minijet-minijet inclusive cross section depends on neither the minijet nor decorrelation momentum, which corroborates the anticipated complete disappearance of the azimuthal decorrelation of jets with the transverse momentum below the saturation scale.

12 Summary and conclusions

We formulated the theory of DIS off nuclear targets based on the consistent treatment of propagation of color dipoles in nuclear medium. What is viewed as attenuation in the laboratory frame can be interpreted as a fusion of partons from different nucleons of the ultrarelativistic nucleus. Diffractive attenuation of color single $q\bar{q}$ states gives a consistent definition of the WW unintegrated gluon structure function of the nucleus [11, 8]. In these lectures we demonstrated how all other nuclear DIS observables - sea quark structure function and its decomposition into equally important genuine inelastic and diffractive components, exclusive diffraction off nuclei, the jet-jet inclusive cross section, - are uniquely calculable in terms of the NSS-defined nuclear WW glue. This property can be considered as a new factorization which connects DIS in the regimes of low and high density of partons.

The two-plateau single parton (jet) inclusive cross section with the strong Q^2 dependence of the plateau for truly inelastic DIS has not been discussed before. A comparison with the initial state nuclear parton densities which evolve from the NSS-defined WW nuclear glue shows an exact equality of the FS and IS parton densities. The plateau-like saturated nuclear quark density is suggestive of the Fermi statistics, but our principal point that for any projectile which interacts weakly with colored partons the saturated density measures the momentum distribution in the $q\bar{q}, gg, \dots$ Fock state of the projectile disproves the Fermi-statistics interpretation. The spin and color multiplet of colored partons the photon couples to is completely irrelevant, what only counts is an opacity of heavy nuclei.

The anti-collinear splitting of WW nuclear glue into soft sea partons is a noteworthy feature of the both diffractive DIS and IS sea parton distributions. The collective nuclear WW gluon field exhibits strong nuclear suppression, and the emergence of a saturated density of sea partons from the nuclear-diluted WW glue is due to the nuclear broadening of the plateau. Because the predominance of diffraction is a very special feature of DIS [2], one must be careful with applying the IS parton densities to, for instance, nuclear collisions, in which diffraction wouldn't be of any significance. The anti-collinear splitting of WW nuclear glue is a clearcut evidence for inapplicability of the DGLAP evolution to nuclear structure functions unless $Q^2 \gg Q_{8A}^2$.

Although in our derivation we focused on DIS, all the results for hard single-jet and jet-jet inclusive cross sections are fully applicable to production of jets in the beam fragmentation region of meson-nucleus collisions and can readily be extended to nucleon-nucleus collisions. Indeed, as argued in [11], the final state interaction between the final state quark and antiquark can be neglected and plane-wave approximation becomes applicable as soon as the invariant mass of the dijet exceeds a typical mass scale of prominent meson

resonances.

Of particular interest are the results on the azimuthal decorrelation of hard jets, in particular, disappearance of azimuthal jet-jet correlations of minijets with momenta below the saturation scale. For the average DIS on heavy nuclei we estimate $Q_{8A}^2 \approx 2 \text{ GeV}^2$, but for the central DIS at a small impact parameter the saturation scale can be several times larger. For instance, from peripheral DIS to central DIS on a heavy nucleus like Pt , ν_{8A} rises from $\nu_{8A} = 1$ to $\nu_{8A} \sim 13$, so that according to (113) a probability to find the away jet decreases by the large factor ~ 3.5 from peripheral to central DIS off Pt target.

The early experience with application of color dipole formalism to hard hadron-nucleus interactions [21] suggests that our analysis can be readily generalized to mid-rapidity jets. One only has to choose an appropriate system of dipoles, for instance, the open heavy flavor production can be treated in terms of the intranuclear propagation of the gluon-quark-antiquark system in the overall color-singlet state. For this reason, we expect similar strong decorrelation of mid-rapidity jets in hadron-nucleus and nucleus-nucleus collisions. To this end, recently the STAR collaboration reported a disappearance of back-to-back high p_\perp hadron correlation in central gold-gold collisions at RHIC [17]. Nuclear enhancement of the azimuthal decorrelation of the trigger and away jets discussed in sections 10 and 11 may contribute substantially to the STAR effect. Here we emphasize that we discuss the distortions of the produced jet-jet inclusive spectrum due to interactions with the nucleons of the target, a practical consideration of azimuthal decorrelations in central heavy ion collisions must include rescatterings of parent high- p_\perp partons on the abundantly produced secondary hadrons.

This work has been partly supported by the INTAS grants 97-30494 & 00-00366 and the DFG grant 436RUS17/89/02.

References

- [1] N.N. Nikolaev and V.I. Zakharov, *Sov. J. Nucl. Phys.* **21** (1975) 227; *Yad. Fiz.* **21** (1975) 434; *Phys. Lett.* **B55** (1975) 397.
- [2] N.N. Nikolaev, B.G. Zakharov and V.R. Zoller, *Z. Phys.* **A351** (1995) 435.
- [3] N.N. Nikolaev, In: *Elementary Particle and Nuclear Physics*. Leningrad Institute of Nuclear Physics Publ., 1976. v.2, pp. 95-146.
- [4] N.N. Nikolaev, *Uspekhi Fiz. Nauk* **134** (1981) 369; *Sov. Phys. Uspekhi* **24** (1981) 531
- [5] N.N. Nikolaev and B.G. Zakharov, *Z. Phys.* **C49** (1991) 607
- [6] A.H. Mueller, *Nucl. Phys.* **B335** (1990) 115.
- [7] L. McLerran and R. Venugopalan, *Phys. Rev.* **D49** (1994) 2233; **D55** (1997) 5414; E. Iancu, A. Leonidov and L. McLerran, Lectures at the Cargèse Summer School, August 6-18, 2001, [arXiv:hep-ph/0202270](https://arxiv.org/abs/hep-ph/0202270).
- [8] N.N. Nikolaev, W. Schafer, B.G. Zakharov, V.R. Zoller. *JETP Lett.* **76** (2002) 195.
- [9] N.N. Nikolaev and B.G. Zakharov, *Z. Phys.* **C53** (1992) 331.
- [10] N.N. Nikolaev and B.G. Zakharov, *Phys. Lett.* **B332** (1994) 177.
- [11] N.N. Nikolaev, W. Schäfer and G. Schwiete, *JETP Lett.* **72** (2000) 583; *Pisma Zh. Eksp. Teor. Fiz.* **72** (2000) 583; *Phys. Rev.* **D63** (2001) 014020.
- [12] N.N. Nikolaev and B.G. Zakharov, *J. Exp. Theor. Phys.* **78** (1994) 806; [*Zh. Eksp. Teor. Fiz.* **105** (1994) 1498]; *Z. Phys.* **C64** (1994) 631.
- [13] V. Barone, M. Genovese, N.N. Nikolaev, E. Predazzi and B.G. Zakharov. *Phys. Lett.* **B326** (1994) 161
- [14] M. Genovese, N.N. Nikolaev and B.G. Zakharov, *J. Exp. Theor. Phys.* **81** (1995) 633; [*Zh. Eksp. Teor. Fiz.* **108** (1995) 1155]
- [15] N.N. Nikolaev, W. Schafer, B.G. Zakharov, V.R. Zoller, paper in preparation.
- [16] A. Szczurek, N.N. Nikolaev, W. Schafer, J. Speth, *Phys. Lett.* **B500**, 254 (2001)
- [17] C. Adler, et al. (STAR Collaboration), E-print Archive: [nucl-ex/0210033](https://arxiv.org/abs/nucl-ex/0210033)
- [18] N.N. Nikolaev, B.G. Zakharov and V.R. Zoller, *JETP Lett.* **59** (1994) 6

- [19] N.N. Nikolaev and B.G. Zakharov. *Phys. Lett.* **B332** (1994) 184
- [20] N.N. Nikolaev, J. Speth, B.G. Zakharov, *J. Exp. Theor. Phys.* **82** (1996) 1046; *Zh. Eksp. Teor. Fiz.* **109** (1996) 1948
- [21] N.N. Nikolaev, G. Piller and B.G. Zakharov. *J. Exp. Theor. Phys.* **81** (1995) 851; *Z. Phys.* **A354** (1996) 99
- [22] B.G. Zakharov, *JETP Lett.* **63** (1996) 952; *JETP Lett.* **65** (1997) 615; *Phys. Atom. Nucl.* **61** (1998) 838;
- [23] V.R. Zoller, *Z. Phys.* **C51** (1991) 659; M.A. Faessler, *Z. Phys.* **C58** (1993) 567.
- [24] T.Akesson et al. (HELIOS Collab.), *Z. Phys.* **C49** (1991) 355
- [25] L.D. Landau and I.Ya. Pomeranchuk, *J. Exp. Theor. Phys.* **24** (1953) 505; I.Ya. Pomeranchuk and E.L. Feinberg, *Doklady Akademii Nauk SSSR* **93** (1953) 439
- [26] E.L. Feinberg, *J. Exp. Theor. Phys.* **28** (1955) 242; E.L. Feinberg and I.Ya. Pomeranchuk, *Nuovo Cim. (Suppl.)* **4** (1956) 652
- [27] R.J. Glauber, *Phys. Rev.* **99** (1955) 1515.
- [28] E791 Collaboration, E.M. Aitala et al., *Phys. Rev. Lett.* **86** (2001) 4773, 4768;
- [29] V.L. Chernyak and A.R. Zhitnitsky, *Phys. Rept.* **112** (1984) 173; P. Kroll, πN Newslett. **15**(1999); R. Jakob and P. Kroll, *Phys. Lett.* **B315** (1993) 463 Erratum-ibid. **B319** (1993) G.P. Lepage and S.J. Brodsky, *Phys. Rev.* **D22** (1980) 2157; S.J. Brodsky, H.-C. Pauli and S.S. Pinsky, *Phys. Rept.* **301** (1998) 299.
- [30] I.P. Ivanov and N.N. Nikolaev, *Phys. Atom. Nucl.* **64** (2001) 753; *Yad. Fiz.* **64** (2001) 813; *Phys. Rev.* **D65** (2002) 054004.
- [31] V.L. Chernyak, *Phys. Lett.* **B516** (2001) 116; V.L. Chernyak, A.G. Grozin, *Phys. Lett.* **B517** (2001) 119.
- [32] V.M. Braun, D.Yu. Ivanov, A. Schaefer, L. Szymanowski, *Phys. Lett.* **B509** (2001) 43; *Nucl. Phys.* **B638** (2002) 111.
- [33] L. Frankfurt, G.A. Miller, M. Strikman, *Phys. Lett.* **B304** (1993) 1; *Phys. Rev.* **D65** (2002):094015;
- [34] M. Genovese, N.N. Nikolaev and B.G. Zakharov, *Phys. Lett.* **B378** (1996) 347
- [35] A.H. Mueller, *Nucl. Phys.* **B558** (1999) 285; Lectures at the Cargèse Summer School, August 6-18, 2001, [arXiv:hep-ph/0111244](https://arxiv.org/abs/hep-ph/0111244).
- [36] J. Nemchik, N.N. Nikolaev, B.G. Zakharov, *Phys. Lett.* **B341** (1994) 228
- [37] M. Genovese, N.N. Nikolaev and B.G. Zakharov, *Phys. Lett.* **B380** (1996) 213